PERGAMON

International Journal of Mechanical Sciences 42 (2000) 1715–1752

International Journal of MECHANICAL SCIENCES

www.elsevier.com/locate/ijmecsci

Thermal modeling of the metal cutting process Part I — Temperature rise distribution due to shear plane heat source

R. Komanduri*, Z.B. Hou

Mechanical and Aerospace Engineering, Oklahoma State University, Stillwater, OK 74078, USA

Received 7 October 1998; accepted 3 June 1999

Abstract

The model of an oblique band heat source moving in the direction of cutting, first introduced by Hahn (Proceedings of First U.S. National Congress of Applied Mechanics 1951. p. 661–6) for an infinite medium in 1951 and subsequently modified by Chao and Trigger (Transactions of ASME 1953;75:109–20) in 1953 for a semi-infinite medium, is extended in this investigation by including appropriate image heat sources. It is used for the determination of the temperature rise distribution in the chip and the work material near the shear plane caused by the main shear plane heat source in orthogonal machining of a continuous chip. A new approach is taken in that the analysis is made in two separate parts, namely, the workmaterial side and the chip side of the shear plane and then combined. The workmaterial (or the chip) is extended past the shear plane as an imaginary region for continuity to determine the temperature distribution in the workmaterial (or the chip) near the shear plane. The imaginary regions are the regions either of the workmaterial that was cut by the cutting tool prior to this instance and became the chip or will be cut by the cutting tool prior to becoming the chip. An appropriate image heat source with the same intensity as the shear plane heat source is considered for each case. The temperature distributions in the chip and the workmaterial were determined separately by this method and combined to obtain isotherms of the total temperature distribution (and not merely the average temperatures). It appears that the significance of Hahn's ingenious idea and his general solution have not been fully appreciated; instead, an approximate approach involving heat partition between the chip and the work was frequently used (Trigger and Chao. Transactions of ASME 1951;73:57–68; Loewen and Shaw. Transactions of ASME 1954;71:217–31; Leone. Transactions of ASME 1954;76:121–5; Nakayama. Bulletin of the Faculty of Engineering National University of Yokohama, Yokohama, Japan, 1956;21:1–5; Boothroyd. Proceedings of the Institution of Mechanical Engineers (Lon) 1963;177(29):789–810). It may be noted that in utilizing Hahn's modified solution, it is not necessary to make an explicit a priori assumption regarding partitioning of heat between the workmaterial and the chip, as was common in most prior work. Instead, this information is provided as part of the solution. The results obtained with the exact analysis were compared with other methods using

* Corresponding author. Tel.: 001-405-744-5900; fax: 001-405-744-7873.
E-mail address: ranga@master.ceat.okstate.edu (R. Komanduri).

PII: S0020-7403(99)00070-3

Nomenclature

a	thermal diffusivity, cm^2/s
B	fraction of the shear plane heat conducted into the workmaterial
$(1-B)$	fraction of the shear plane heat conducted into the chip
c	specific heat, J/g°C
F_c	cutting force, N
F_t	feed force, N
F_s	shearing force on the main shear plane, N
F	frictional force at the chip–tool interface, N
l_i	location of the differential small segment of the shear band heat source dl_i relative to the upper end of it and along its width, cm
L	width of the shear band heat source, cm
M	any point in the medium where the temperature rise is concerned
N_{th}	thermal number ($= t_c V_c/a$)
q_l	heat liberation intensity of a moving line heat source, J/cm s
q_{pl}	heat liberation intensity of a moving plane heat source, J/cm^2 s
R	distance between the moving line heat source and the point M, where the temperature rise is concerned, cm
r	chip thickness ratio ($= t_c/t_{chip}$, or V_{ch}/V_c)
t_c	depth of cut, or undeformed chip thickness, cm
V	velocity of a moving plane heat source, cm/s
V_c	cutting speed, cm/s
V_s	shear velocity, cm/s
V_{ch}	chip velocity, cm/s
w	width of cut, cm
X, z	the coordinates of the point where the temperature rise is concerned in the moving coordinate system, cm

Greek letters

α	rake angle, degrees
θ	temperature rise, °C
θ_M	temperature rise at point M,°C
λ	thermal conductivity, J/cm s °C
ρ	density, g/cm^3
ϕ	shear angle, degree
φ	oblique angle, degree

the experimental data available in the literature to point out some of the discrepancies in the simplified models. It may be pointed out that these models assume the temperature rise at the chip–tool interface to be nearly uniform and equals the average temperature rise in this volume. A comparison of the calculated temperature rise by these methods with the exact analysis indicates that the differences can be quite significant ($\sim$ 50% or higher). It is hoped that future researchers would recognize the significance and the versatility of the exact analysis in determining the temperature distribution in the shear zone in metal cutting.

Keywords: Thermal aspects of machining; Moving heat source; Heat partition; Shear plane

1. Introduction

The heat generated in cutting was one of the first and the foremost topics investigated in machining. Pioneering work in this area was due to Benjamin Thompson (Count Rumford) [1], who in 1798 investigated the heat generated in the boring of a cannon and developed the concept of mechanical equivalent of heat, the exact relationship of which was established by Joule in 1850 [2]. Subsequently, Taylor [3] recognized the importance of heat in accelerating tool wear and developed an empirical relationship between the cutting speed (consequently the tool temperature) and the tool life which is still in use today. He also developed a more heat resistant material, termed as the high speed steel (HSS), which is still used extensively in machining not at high speeds but towards the lower end of the cutting speed spectrum. Till the middle of this century, much of the work on the thermal aspects of machining has been mostly experimental, either calorimetric type [4,5], or, using thermocouples to measure the temperatures at various locations in the tool/workmaterial [6,7]. In the late 1930s to mid 1940s, Rosenthal [8], Blok [9], and Jaeger [10] made seminal contributions on the moving heat source problems that formed the basis for much of the analytical investigations of the temperatures generated in machining that followed. Pioneering analytical work on the temperature generated in machining was due to Hahn [11], Chao and Trigger [12], Trigger and Chao [13], and Loewen and Shaw [14]. Other important analytical contributions in this area include the work of Leone [15], Nakayama [16], Boothroyd [17], Weiner [18], Rapier [19], Dutt and Brewer [20], and Dawson and Malkin [21].

Barrow [22] reviewed both theoretical and experimental techniques for assessing the cutting temperatures and may be referred to for details on other contributions. Fig. 1(a)–(h) give a summary of the various models used in the determination of the shear plane temperature in machining. Most assume the material on either side of the shear plane as two separate bodies in sliding contact. Only Hahn [11] and Chao and Trigger [12] assume it correctly as a single body, i.e., the material in front of and behind the heat source is the same. For this reason, other models are considered approximate. The main differences in these models include the assumptions made, such as the nature of the heat source, the estimation of the heat partition ratio, the direction of motion of the heat source, and the boundary conditions. For example, Trigger and Chao [13] assumed the shear plane as the heat source with the work surface and the machined surface as adiabatic boundaries [Fig. 1(a)]. Hahn, on the other hand, used an oblique shear plane heat source moving in the cutting direction with the cutting velocity in an infinite medium [Fig. 1(b)]. Chao and Trigger [12] extended Hahn's model by

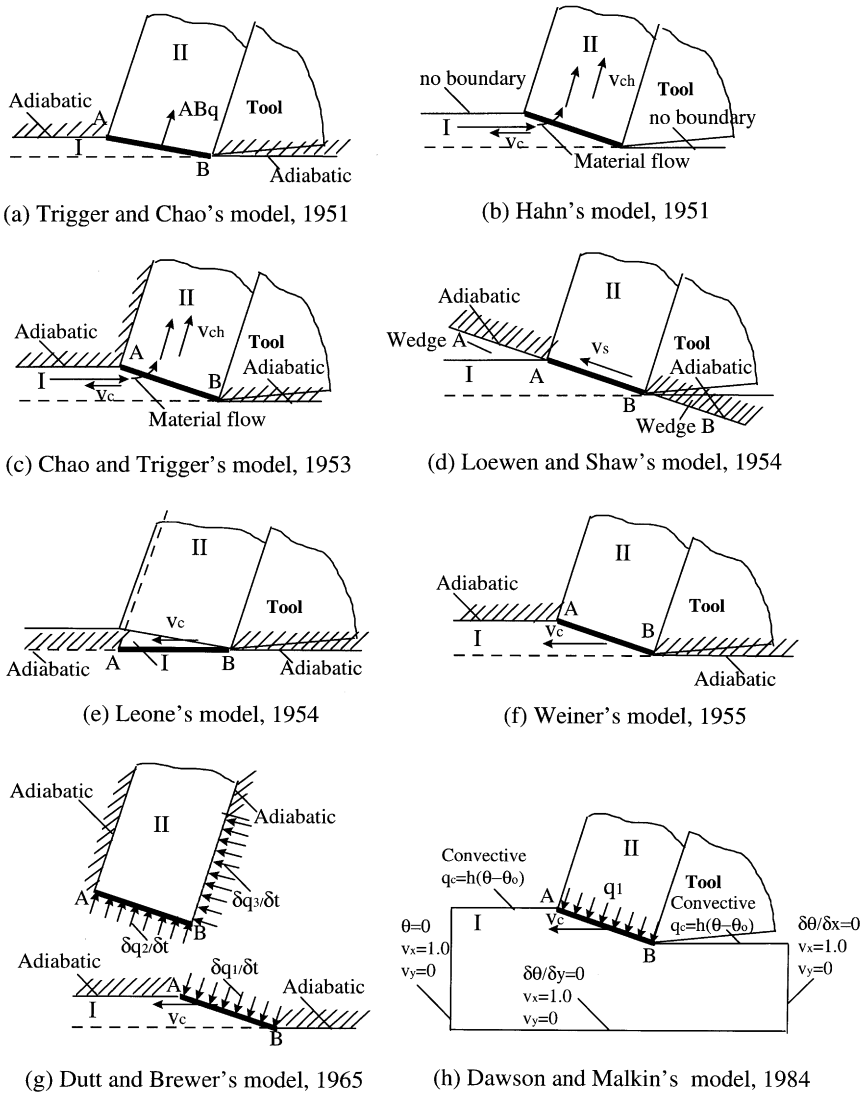

Fig. 1. Summary of the models used by various researchers for the determination of the temperature rise in the chip and workmaterial caused by the shear plane heat source in machining.

considering a semi-infinite medium [Fig. 1(c)] but assumed the temperature at any point to be twice that for an infinite body. This is true only for the special case of the heat source moving entirely on the boundary surface of a semi-infinite body, as will be shown in this investigation. Loewen and Shaw [23], in a discussion to Chao and Trigger [12], pointed out that this would not be correct, for such a model predicts more uniform temperature while in reality the distribution is far from uniform. In the present investigation, this problem was addressed by considering appropriate image sources.

Loewen and Shaw [14] assumed the shear plane heat source to be moving at the velocity of shear instead of the cutting velocity [Fig. 1(d)] based on Piispanen's sliding deck of cards model for the

deformation in the shear zone [24]. However, an approximation is involved in this model in that the metal which is assumed to be present in wedge *A* is not there, while that in the wedge *B* that is present is ignored. Such a model, however, enables the use of Jaeger's solution for the moving slider problem and Blok's heat partition but did not consider material flow. When the later is considered, it would result in the transport of some of the heat that flowed into the workmaterial back into the chip. Since they use heat partition and did not consider the material flow, the fraction of the heat that goes into the chip consequently would be higher than predicted by their model. Leone's [15] model is similar to Loewen and Shaw's [14] but assumed the shear plane heat source to be parallel to the cutting direction (i.e. shear angle zero since it is usually small) moving in the direction of cutting at the cutting velocity [Fig. 1(e)]. Thus, the chip formation process was converted to a frictional sliding contact problem. Both Loewen and Shaw [14] and Leone [15] used Jaeger's solution for the moving slider problem and considered the initial heat partition only, ignoring subsequent heat flow due to mass flow from the work side into the chip. Consequently, *the actual heat partition fraction for the chip would be higher than that obtained by their methods*.

Weiner's model [18] is similar to Loewen and Shaw's [14] in some respects. Winer's inclined shear plane heat source moves at the cutting velocity instead of at the shear velocity as in the case of Loewen and Shaw [Fig. 1(f)]. So, the heat source moves into the workmaterial instead of an imaginary space. Also, while Loewen and Shaw [14] used Jaeger's solution, Weiner started with the partial differential equation of heat conduction but had to make a number of assumptions to solve it including the chip velocity to be perpendicular to the shear plane. As a result, although the calculated results of the fraction of heat going into the chip should be lower than the actual value (similar to Loewen and Shaw), Weiner actually found it to be higher. This is attributed to the many assumptions made in the model including adiabatic boundaries to solve the partial differential equation.

Rapier [19] used relaxation methods to compute the temperature distribution by considering the case of temperature distribution in an infinite body moving perpendicular to the plane heat source. Dutt and Brewer [20] used finite difference methods [Fig. 1(g)] and established generalized equations for the chip, the workmaterial, and the tool as separate entities and combined via the conditions at the interface into equations valid throughout the system as a whole. A self-determination principle was used to establish the boundary conditions. Tay et al. [25] determined the temperature distribution in orthogonal machining using the finite element method (FEM). Dawson and Malkin [21] extended Weiner's model by modifying the boundary conditions, namely, convective boundaries instead of adiabatic and used finite element analysis to determine the temperature distribution [Fig. 1(h)].

As pointed out earlier, most of the earlier models (except Hahn's [11] and Chao and Trigger's [12]), considered the deformation in the shear zone as two bodies in sliding contact and used heat partition, an ingenious approach originally introduced by Blok [9] for the evaluation of the average temperature at the interface between two bodies in sliding contact. In Blok's model, of the two bodies in relative motion, one is stationary and the other moves with the relative velocity. While it is logical to consider heat partition at the chip–tool interface as two bodies in relative sliding, namely, the sliding chip and the stationary tool are involved, such an approach hardly seems valid (and not necessary as will be shown in this investigation) in the case of shear zone as there is only one body involved, namely, the work material deforming plastically at the shear zone to form the chip. In spite of it, the partitioning approach has been used by some researchers in the analysis of the temperature rise in the shear zone to enable the use of Jaeger's solution.

The heat partition approach for the shear plane heat source is at best approximate and need not be used since an exact analytical solution is available (for, e.g., [11,12]). Also, the use of average temperature at the shear zone for the heat partition, though convenient, is not accurate as the temperature varies throughout the length of the shear plane from the tool tip to the chip–workmaterial intersection, as will be shown in this investigation. Also, major concentration of efforts was on the determination of the average temperature instead of the temperature distribution. The latter is accomplished in this investigation for the first time by exact analysis. However, this has to be solved numerically which is computationally intensive. The lack of computational power in the early 1950s appears to be the main reason why Hahn [11] and soon thereafter by Chao and Trigger [12] did not determine the temperature distribution in the chip and workmaterial near the shear zone. But with the advent of rather inexpensive, powerful computers, this no longer is a limitation. However, the variation of thermal properties with temperature cannot be taken into account due to the complexity involved in the analytical method and consequently only average values are taken.

This paper focuses on the temperature distribution near the shear zone, both in the chip and the workmaterial, incorporating appropriate image sources. This overcomes Loewen and Shaw's [23] concern for the Chao and Trigger's model [12]. The shear plane is considered as an infinitely long oblique plane heat source moving with the cutting velocity. The work material is extended past the shear zone as an imaginary area for convenience [Fig. 2(a)] to determine the temperature rise distribution in the workmaterial. Similarly, the chip is extended into the workmaterial past the shear plane as an imaginary area for convenience [Fig. 2(b)] to determine the temperature rise distribution in the chip. The temperature distributions on the imaginary sides are not valid and hence are not taken into consideration. In this three-part series, the temperature rise distribution due to the shear plane heat source only is considered in Part I, the frictional heat source at the chip–tool interface considering varying heat partition and matching the temperatures on the chip side and the tool side using functional analysis approach [26] in Part II, and the combined effect of the heat sources, namely, shear plane heat source and the frictional heat source at the tool–chip interface [27] in Part III.

2. Review of the literature

In the following, a detailed review of the prior modeling of the thermal partitioning of heat generated in the shear plane during metal cutting process is presented. It may be noted that in the early 1950s, many of the papers (especially in the ASME transactions) dealing with the thermal aspects of machining had detailed discussions by such outstanding researchers as Trigger, Chao, Loewen, Shaw, Blok, Hahn, Merchant, to name a few. In fact, some discussions were longer than the original papers. Unfortunately, the significance of these contributions are often overlooked and hence an attempt was made here to capture them.

Trigger and Chao [13] in 1951, presented an analytical method for the evaluation of the metal cutting temperatures that marked the beginning of a glorious chapter on the modeling of the cutting temperatures in machining. Their contributions in the decade following had addressed many important thermal problems in machining. Trigger and Chao [13] determined the average chip temperature as it leaves the shear zone by considering the total mechanical energy input as

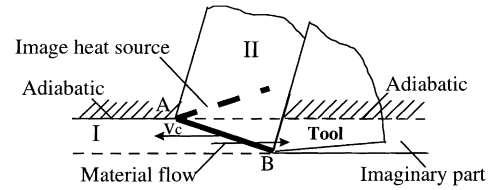

(a) model for thermal analysis of work

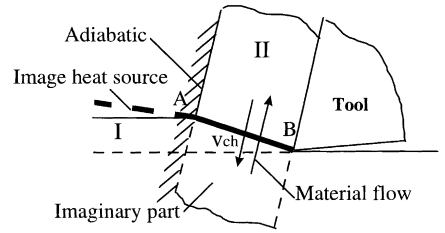

(b) model for thermal analysis of chip

(Komanduri and Hou's model)

Fig. 2. Modified Hahn's models for the determination of the temperature rise in the chip and workmaterial, caused by the shear plane heat source in machining.

well as the shear energy at the shear plane. Based on the work of Schmidt and Roubik [5], they assumed the heat partition into the chip to be 90% and that in the work to be 10%. They also assumed that of the total plastic deformation energy, some 12.5% would remain in the deformed chip as latent energy based on the work of Taylor and Quinney [28]. However, other researchers chose to neglect this part in their analyses as it is considered to be small (or negligible) and unknown.

Trigger and Chao [13] calculated the average temperature rise of the chip as it leaves the shear plane due to the shear plane heat source using the equation:

$$\bar{\theta}_s = \frac{A[F_c V_c(1-B) - FV_{ch}]}{Jc\rho V_c tw}. \tag{1}$$

Here, $\bar{\theta}_s c\rho V_c tw$ is the increment of internal heat energy in the material passing through the shear plane heat source per unit time and $A[F_c V_c(1-B) - FV_{ch}]$ is the sensible heat part of the work done from the shearing process in the shear band per unit time, and J is the Joule's mechanical equivalent of heat. The reason for considering the average temperatures was because the available experimental techniques only yielded average temperatures. Trigger and Chao considered the heat liberation intensity to be uniformly distributed. Consequently, the temperature distribution would be uniform in the chip so long as there is no heat loss. Thus the temperature rise along the shear plane, $\bar{\theta}_s$ would also be uniform. B is the heat partition into the workmaterial and $(1-B)$ into the chip. A is the percentage of the total shearing deformation energy appearing as sensible heat (87.5%) and $(1-A)$ is stored in the deformed chip material as latent energy. Trigger and Chao [13]

considered the heat generated at the shear zone as well as at the chip–tool interface. They calculated the average temperature at the chip–tool interface and compared it with the experimental results and found reasonably good agreement.

Since the pioneering work of Trigger and Chao in 1951, the problem of heat partition was widely considered. Many neglected the contribution due to latent energy stored in the deformed chip during machining. Thus, [Eq. (2)] is widely used [instead of Eq. (1)] for the estimation of the average temperature rise in the chip due to shear plane heat source.

$$\bar{\theta}_s = (1 - B)\frac{(F_c V_c - F V_{ch})}{J c \rho V_c t w} \tag{2}$$

where $F_s V_s = (F_c V_c - F V_{ch})$. Loewen and Shaw [14] considered the chip and the workmaterial as two bodies in relative motion (imaginary) at the shear plane. Relative to the shear plane, the chip was considered as a stationary body and the workmaterial as a moving body moving in the direction of the shear plane. Thus, the heat transfer problem in chip formation was considered to be equivalent to that of a sliding contact and Blok's [9] ingenious heat partition principle commonly used in tribology was applied. Thus the average temperature rise at the shear plane calculated on the chip side, based on a stationary plane heat source model, should be equal to that at the workmaterial side using the moving heat source model. From that the heat partition fractions for the workmaterial (B) and for the chip ($1 - B$) are calculated [14]. The average temperatures on either side of the shear plane are calculated using the solutions of stationary and moving plane heat sources after Carslaw and Jaeger [10,29].

Blok, in a discussion to Loewen and Shaw [14], questioned the validity of the application of the principle of heat partition to the problem of the shear plane heat source. He pointed out that in the shear plane problem, material is subjected to motion across the heating surface (the shear plane) and this motion induces heat to be carried away by convection across the surface. Thus, in so far as the moving material, and thus the convection of heat is concerned, a real partition cannot be effected. This means one should consider both heat and mass transfer effects. He even proposed a simplified model of the shear plane heat source with a mirror image for a semi-infinite system. It may be noted that the image sources are different for the chip side and the workmaterial side. Unfortunately, a solution for this model was not available at that time due to complexity involved in the analysis and non availability of computers readily. The model proposed in the present investigation has some features similar to Blok's model with the main difference being that separate models were considered for the shear plane heat source from the work material side and the chip side, respectively and combined to obtain the temperature distribution in the workmaterial and the chip. This way, the analytical solution was obtained.

Actually, the chip and the workmaterial are not two separate bodies in contact. This is a material flow process in which a certain amount of the workmaterial continuously flows through the shear plane to form the chip. Of the heat carried to the workmaterial, Bq, a part flows back into the chip. It appears that without appropriate compensation for the heat transfer caused by the flow of the heat carrying material, the value B (or $1 - B$) calculated based on the Blok's heat partition principle for the temperature rise calculations in metal cutting would be in error. Material flow of the workmaterial to the chip is totally a different process than sliding contact between two bodies. Thus the assumption of equating the two totally different processes, as Blok rightly pointed out, is somewhat questionable.

Table 1
Equations for the determination of B and $(1-B)$

Source	Equation for the determination of B
Trigger and Chao [13]	$B = 0.1$
Loewen and Shaw [14]	$(1-B) = 1\Big/\left(1 + 1.328\sqrt{\frac{a\gamma}{v_c t_c}}\right)$
Leone [15]	$B = 1\Big/\left(1 + 1.13r\sqrt{\frac{Lv_c}{a}}\right)$
Boothroyd [17]	$B = f(N_{th}\tan\phi)$[a]

[a]Boothroyd used Weiner's (1955) equation as given below

$$B = \frac{1}{4Y_L}\mathrm{erf}(\sqrt{Y_L} + (1 + Y_L)\mathrm{erf}\, c\sqrt{Y_L} - \frac{e^{-Y_L}}{\sqrt{\pi}}\left(\frac{1}{2\sqrt{Y_L}} + \sqrt{Y_L}\right)$$

where $Y_L = (v_c t_c/4a)\tan\phi = (N_{th}/4)\tan\phi$, ϕ is the shear angle, N_{th} is the thermal number, $N_{th} = v_c t_c/a$.

Table 1 is a summary of the equations used for the heat partition fraction B (or $1-B$) by various researchers. Trigger and Chao [13] assumed a constant value for the heat partition ($B = 0.1$) while Leowen and Shaw introduced the effect of thermo-mechanical properties of the workmaterial as well as the cutting conditions in the heat partition fraction. Boothroyd [17] used Weiner's [18] equation. It may be noted that Boothroyd used *depth of cut* as the length parameter in the *Thermal Number*, N_{th} while *the length* (*or half length*) *of the heat source* is used as the length parameter in *Peclet or Jaeger Number*. Boothroyd [17,30] developed a plot showing the variation of $N_{th}\tan\phi$ with the fraction of the shear plane heat conducted into the workmaterial, B and compared it with his experimental data as well as that of Nakayama's [16] (Fig. 3). Comparing the theoretical plot with the experimental results, it can be seen that the experimental values are much higher, especially when $N_{th}\tan\phi > 3$, i.e., when the thermal number is high (say, $N_{th} > 8$) *the fraction of the heat going into the chip* $(1-B)$ (*and consequently the average temperature rise*) *is estimated to be higher. Larger the* N_{th}, *the higher the estimated average temperature rise in the chip and higher the differences between the theoretical and experimental values. When the* N_{th} *is low* (< 4), *the theoretical value of* B *or* $(1-B)$ *is closer to the experimental values.*

Dawson and Malkin [21] extended Weiner's model by modifying the boundary conditions from adiabatic to convective [Fig. 1(h)]. Fig. 4 is the variation of heat flow into the chip $(1-B)$ with $4L\sin\phi\tan\phi$. Weiner's [18] analytical results as well as Boothroyd's [17] and Nakayama's [16] experimental results are included along with Dawson and Malkin's [21] analytical results. It can be seen that the experimental values of $(1-B)$ are much lower than predicted.

Trigger and Chao considered a constant value of heat partition ($B = 0.1$) based on conventional machining of steel. Their results are closer to the values determined by the exact solutions reported here for steels (compared to simplified analytical equations) but not for other materials. Since some

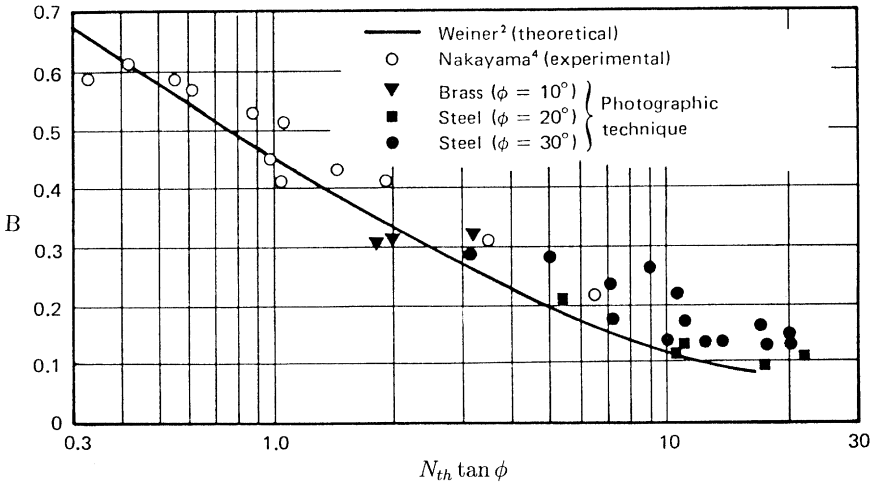

Fig. 3. Effect of N_{th} tan ϕ on the partition of shear plane heat between the chip and the workpiece (after Boothroyd [30]). B — fraction of the shear plane heat conducted into the workpiece N_{th} — thermal number; ϕ — shear angle.

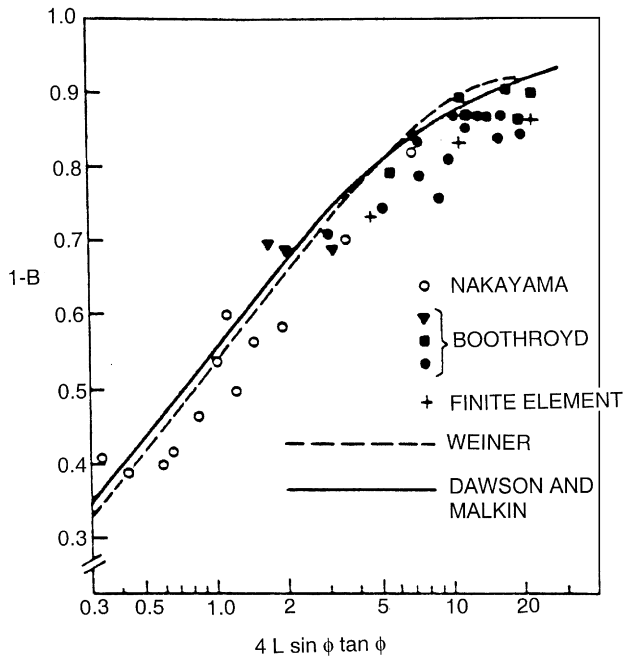

Fig. 4. Effect of $4L \sin \phi \tan \phi$ on the partition of shear plane heat between the chip and the workpiece (after Dawson and Malkin [21]) L — Peclet or Jaeger number; ϕ — shear angle; $(1 - B)$ — fraction of the shear plane heat conducted into the chip.

models incorporate thermal properties and cutting conditions, it appears that they should be applicable in principle for a range of workmaterials and cutting conditions. But because of simplifying assumptions, they can differ significantly from the exact solutions.

3. Proposed model

Instead of using simplified models to avoid compensation for the flow of heat carrying material, Hahn [11] embarked on a totally new direction for the analysis of the shear plane heat source without the need for heat partition. He used an oblique moving band heat source model based on the true nature of the chip formation process. In cutting, the depth of the layer removed from the workmaterial passes continuously through the shear plane thereby undergoing extensive plastic deformation to form the chip. Hence, the shear plane can be considered as a band heat source moving in the workmaterial obliquely at the velocity of cutting. Unfortunately, as Chao and Trigger [12] pointed out, Hahn [11] only included the high points of his mathematical analysis while details would be valuable to researchers with a less mathematical background. Also, generally the data given is not the components of the moving velocity along X-, and z-axes (V_x and V_z) (as Hahn used in his analysis) but the moving velocity V and the oblique angle φ. Further, in order to verify that the analysis developed here is essentially the same as Hahn's model, one needs to compare them with Hahn's final results starting the analysis from first principles. While Hahn solved his equation starting from the available solution for an *infinitely long instantaneous line heat source* from Carslaw and Jaeger [29], in this paper, we begin from the available solution for an *infinitely long moving line heat source*, namely, Eq. (3) given in the following.

3.1. Analysis of an oblique band heat source moving in the direction of cutting in an infinite medium (*after Hahn* [11])

Fig. 5 shows schematically the shear band heat source moving obliquely at an angle φ with a velocity V in an infinite medium with a heat liberation intensity of q_{pl} (J/cm^2 s). The band heat source is infinitely long of width $2l$. A moving coordinate system is considered with its oX-axis along the width of the plane of the moving band heat source and its origin o coinciding with the mid point. The objective is to determine the temperature rise at any point M at any time t caused by this moving band heat source. The location of the point M (Fig. 5) is expressed by the coordinates in the moving coordinate system at time t.

The moving band heat source is considered as a combination of infinitely small differential segments $\mathrm{d}l_i$, each of which is considered as an infinitely long moving line heat source. Thus, the solution for an infinitely long moving line heat source in an infinite medium [8,10] can be used for calculating the temperature rise at any point M caused by a differential segment $\mathrm{d}l_i$.

$$\theta_M = \frac{q_l}{2\pi\lambda} \mathrm{e}^{-XV/2a} K_0(RV/2a). \tag{3}$$

(See Nomenclature for the definition of the variables.) The distance X is the projection of the distance R in the direction of motion. Eq. (3) is the solution for quasi-steady-state conditions involving long heating times ($t \to \infty$). Consequently, the temperature rise around the heat source will be time independent. Since quasi-steady conditions are reached in ~ 0.1 s for continuous chip formation, Eq. (3) can be used as the basis for the thermal analysis of the metal cutting process.

Consider a segmental moving line heat source (refer to Fig. 5). Using Eq. (3), the heat liberation intensity of this heat source q_l is $q_{pl}\,\mathrm{d}l_i$. The distance R between the line heat source and the point

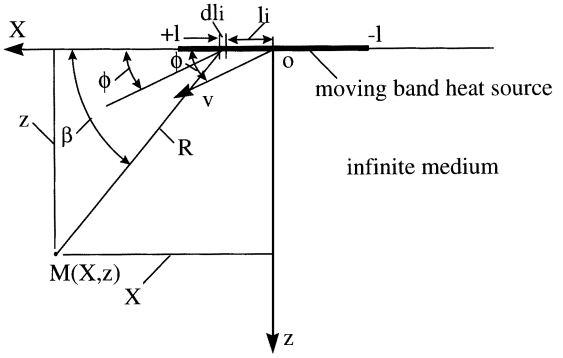

Fig. 5. Schematic of Hahn's model of a band heat source moving obliquely in an infinite medium [11].

M is $\sqrt{(X-l_i)^2+z^2}$, and the projection of this distance in the direction of motion is $R\cos(\beta-\phi)$ (where $\beta=\sin^{-1}(z/R)$). The temperature rise at point M caused by this segmental line heat source is given by

$$\mathrm{d}\theta_M=\frac{q_{pl}\,\mathrm{d}l_i}{2\pi\lambda}\,\mathrm{e}^{-VR\cos(\beta-\phi)/2a}K_0\left(\frac{VR}{2a}\right). \tag{4}$$

Thus, the temperature rise at point M caused by the entire moving band heat source is given by

$$\theta_M=\frac{q_{pl}}{2\pi\lambda}\int_{-l}^{+l}\mathrm{e}^{-VR\cos(\beta-\phi)/2a}K_0\left(\frac{VR}{2a}\right)\mathrm{d}l_i \tag{5}$$

when $z=0$ (i.e., only temperature rise at the heat source is considered), $\beta=0$, $\cos(\beta-\phi)=\cos\phi$, $R=X-l_i$. Thus

$$\theta_M=\frac{q_{pl}}{2\pi\lambda}\int_{-l}^{+l}\mathrm{e}^{-V(X-l_i)\cos\phi/2a}K_0\left[\frac{V(X-l_i)}{2a}\right]\mathrm{d}l_i. \tag{6}$$

Hahn defined $V\cos\phi=V_x$, $1/\cos\phi=\alpha$, $V_xX/2a=\mathbf{X}$, $V_xl/2a=L$.

Substituting them in Eq. (6), we get

$$\theta_M=\frac{q_{pl}}{2\pi\lambda}\int_{-l}^{+l}\mathrm{e}^{-V_x(X-l_i)/2a}K_0\left[\frac{V(X-l_i)}{2a}\right]\mathrm{d}l_i. \tag{7}$$

For using non-dimensional variables, let

$$\frac{V_x(X-l_i)}{2a}=u,\quad \mathrm{d}l_i=-\frac{2a}{V_x}\mathrm{d}u,\quad \frac{V(X-l_i)}{2a}=\frac{u}{\cos\phi}=\alpha u$$

when $l_i=-l$, $u=V_x(X+l)/2a=\mathbf{X}+L$; and when $l_i=+l$, $u=V_x(X-l)/2a=\mathbf{X}-L$. Eq. (7) can be written as

$$\theta_M=\frac{q_{pl}a}{\pi\lambda V_x}\int_{\mathbf{X}-L}^{\mathbf{X}+L}\mathrm{e}^{-u}K_0[\alpha u]\,\mathrm{d}u. \tag{8}$$

Generally, the data given is not the components of the moving velocity along X-, and z-axes, (V_x and V_z) (as Hahn used in his paper) but the moving velocity V and the oblique angle φ. For solving Eq. (6), the following alternative substitutions are made to change the variables into non-dimensional. Let

$$\frac{V(X-l_i)}{2a}=u,\quad \mathrm{d}l_i=-\frac{2a}{V}\,\mathrm{d}u,\quad \frac{VX}{2a}=\mathbf{X},\quad \frac{Vl}{2a}=L$$

when $l_i=-l$, $u=V(X+l)/2a=\mathbf{X}+L$; and when $l_i=+l$, $u=V(X-l)/2a=\mathbf{X}-L$. Eq. (6) can be written as

$$\theta_M=\frac{q_{pl}a}{\pi\lambda V}\int_{\mathbf{X}-L}^{\mathbf{X}+L}\mathrm{e}^{-u\cos\phi}K_0[u]\,\mathrm{d}u. \tag{8'}$$

Eqs. (5) and (8) are solutions for a band heat source moving obliquely in an infinite medium as given by Hahn [11]. Eq. (8′) is basically the same as Eq. (8) but expressed with different initial data. The integral part of Eq. (8′) is a non-dimensional temperature rise due to oblique moving band heat source and is given by

$$\begin{aligned}\frac{\pi\lambda v}{q_{pl}a}\theta_M&=\int_{\mathbf{X}-L}^{\mathbf{X}+L}\mathrm{e}^{-u\cos\phi}K_0[u]\,\mathrm{d}u\\&=\int_{\mathbf{0}}^{\mathbf{X}+L}\mathrm{e}^{-u\cos\phi}K_0[u]\,\mathrm{d}u-\int_{\mathbf{0}}^{\mathbf{X}-L}\mathrm{e}^{-u\cos\phi}K_0[u]\,\mathrm{d}u.\end{aligned} \tag{9}$$

For $\phi=0$ (refer to Fig. 5), this model is the same as Jaeger's [10] and Eq. (9) is the same as Jaeger's Eq. (8) [10]. Thus, Jaeger's solution for a band heat source moving in a direction *parallel* to the plane of the heat source is a special case of Hahn's general solution. Similarly, it will be shown later that Rosenthal's solution [8] for a band heat source moving in a direction *perpendicular* to the plane of the heat source is also a special case of Hahn's general solution. Thus, Hahn's solution is the general solution for an oblique moving heat source.

For ease of application, the two similar integrals in Eq. (9) are each considered as a special function and defined as follows:

$$\int_{u=0}^{u=p}\mathrm{e}^{-u\cos\phi}K_0[u]\,\mathrm{d}u=i(p,\cos\phi)$$

Fig. 15 (see Appendix A) is a plot of this special function showing the variation of $i(p,\xi)$ with p for various values of ξ and Tables 8(a) and (b) give values of this special function $i(p,\xi)$ for various values of $p<0$ [Table 8(a)] and $p>0$ [Table 8(b)]. Using Eq. (8′) and the plots shown in Fig. 15 or the functional values from Table 8, the non-dimensional temperature rise distribution on the oblique moving band heat source can be calculated. It can be seen (from Fig. 15 or Table 8) that when $\xi=1.0$ ($\cos\phi=1$, $\phi=0^\circ$) (the case investigated by Jaeger), the relevant curve and the data is the same as that given by Jaeger [10].

Using Eq. (5), the temperature rise at any point around the oblique moving band heat source (including those points on the heat source) can be calculated. But this involves a complex

integration which can be solved only numerically. The availability of powerful, inexpensive computers today facilitates this greatly. But in the early 1950s, when Hahn considered the oblique moving band heat source problem, computers were not available. Hence, Hahn had to limit his calculations for the temperature rise due to shear plane heat source only for the case where $z = 0$ (refer to Fig. 5). Based on this simplification, Eq. (8) was derived for the case of an infinite medium. In metal cutting, the shear band heat source moves along the boundary with one edge at the boundary all the time. Hence, it is more realistic to consider the conduction medium as semi-infinite. Under the same heat intensity, the temperature rise around the heat source is always higher with a boundary than without. Thus, the results of calculation using Eq. (8) (the solution for an infinite body based on Hahn's model) for the temperature rise due to the shear band heat source appears lower than it should be.

In cutting dry (no lubricant), the boundary upon the shear band is usually considered adiabatic. Thus, for the case where angle φ (refer to Fig. 5) is zero and the band heat source is moving on the boundary of a semi-infinite medium, the problem is simple to solve, i.e., multiplying the solution for an infinite medium by two, as Jaeger did in his analysis. For the general case of moving oblique band heat source, it is necessary to consider an image heat source relative to the existing boundary with the same heat intensity as the primary heat source. Thus Eq. (5) becomes indispensable. However, it is not easy to conduct numerical computation of this complex integral without a computer. This, again, appears to be the reason why Hahn did not present his results involving an oblique moving band heat source in a semi-infinite medium. Jaeger, on the other hand, was able to solve this only for the special case ($\varphi = 0$) of an oblique band heat source moving in a semi-infinite medium, which is widely used in the thermal analysis of sliding contacts.

For application to metal cutting, Trigger and Chao modified Hahn's obliquely moving band heat source model for the case of a semi-infinite medium [13]. They derived the solution starting from the available solution for an *instantaneous line heat source of infinite length*. Considering a semi-infinite medium, they merely multiplied the solution of an instantaneous line heat source by two. Such a consideration is true only for the case where all the heat source is lying on the boundary, which is the case Jaeger considered for the sliding contact problems, but not for the case of metal cutting with an obliquely moving band heat source, in which only one edge of the heat source is on the boundary and the remaining part is under the boundary surface in the depth of cut region. Thus, their solutions are similar to Eq. (5) (the general case for the temperature rise calculations for any point around the heat source) and Eq. (8) (the special case only for the temperature rise on the heat source) but two times higher. So, they technically had not solved the problem of obliquely moving band heat source in a semi-infinite medium for the case of metal cutting.

When we review Hahn's pioneering work in the 1950s, in light of today's advancements in the computational area, it is clear that his equation [Eq. (5)] can easily be solved to determine the distribution of the temperature rise at any point around the oblique moving band heat source. Each calculation for the temperature rise at any point would hardly take a fraction of a second or less. For a complete map of the temperature field in the chip or the workmaterial (usually more than 1000 data points of the temperature rises are needed), the computation time would be ~ 1 to 2 min. By applying Eq. (5) to analyze the thermal effects of the shear band heat source in machining, critical information hitherto difficult to obtain can be obtained. This includes the temperature at

individual locations of importance, the temperature distribution on any plane, the temperature at all points over the area of interest, isotherms of the critical temperatures in the area of interest, average temperatures at relevant areas, etc. In contrast, the approximate methods can provide only the average temperatures and that too may involve considerable error. It can also be seen that it would be difficult, if not impossible, to study important phenomena, such as the mechanism of shear localization in high-speed and ultra high-speed machining without the use of the oblique moving band heat source. Hahn's model thus enables detailed studies of the thermal analysis in machining.

In the obliquely moving band heat source model, the material in front of and behind the heat source are considered as one continuous body. Thus, the heat transfer by conduction and that due to material flow are considered simultaneously. Consequently, this model is much closer to the true nature of the chip formation process in machining. The accompanying heat transfer process can be considered as a shear plane heat source (a band heat source) moving continuously and obliquely in the surface layer (depth of cut) of the workmaterial with the cutting velocity V_c [see Fig. 6(a) and its equivalent Fig. 6(a′)] or as the shear plane heat source moving continuously and obliquely in the chip with a chip flow velocity V_{chip} [see Fig. 6(b) and its equivalent Fig. 6(b′)]. In Fig. 6(a′), it is considered as a band heat source $\overline{\mathbf{oc}}$ obliquely moving under the surface $\overline{\mathbf{aoe}}$ of a semi-infinite body with a velocity V_c where the part of the surface material **eocd** is imaginary and is extended for continuity. Its actual form and location is shown as II in the same schematic. In Fig. 6(b′), it is considered as a band heat source moving in the chip under the surface $\overline{\mathbf{aoe}}$ of a semi-infinite body with a velocity V_{chip} where the part of the chip material **eocd** is imaginary and is again extended for continuity. Its real form and location is shown as I in the same schematic.

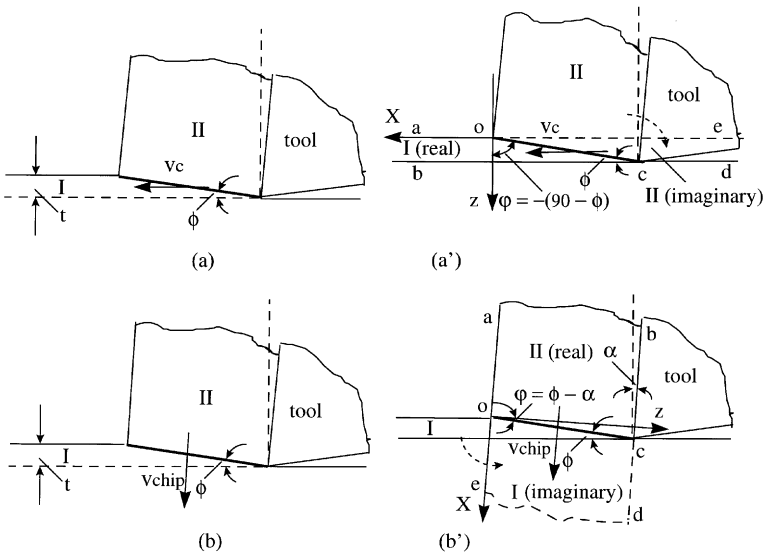

Fig. 6. Schematic of the moving oblique band heat source model for the continuous chip formation process in metal cutting using modified Hahn's model.

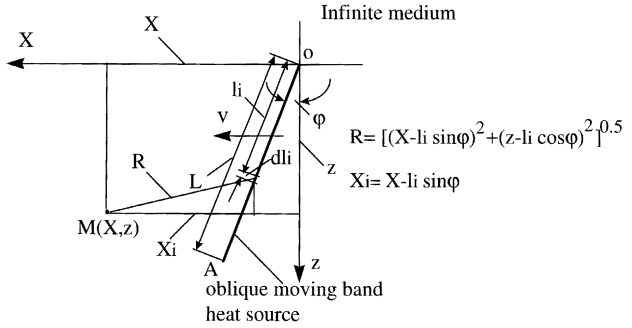

Fig. 7. Schematic of an oblique moving band heat source in an infinite medium.

3.2. Modification of Hahn's solution for an oblique band heat source moving in an infinite medium using an alternative coordinate system with one of its axes in the direction of motion

Hahn derived the general equation for a band heat source moving obliquely in an infinite medium. This equation has to be modified further for application to a semi-infinite body for the oblique moving shear plane heat source as outlined in the following.

For ease of derivation of the equation for an oblique moving heat source in a semi-infinite medium, based on Hahn's original work, an alternative moving coordinate system is considered. Referring to Fig. 7, the X-axis of the moving co-ordinate system is in the direction of the motion, the origin o of which coincides with one end of the band heat source oA, and angle φ is defined as the oblique angle (the angle between the heat source and the z-axis). Actually Fig. 7 shows the same heat transfer model of the band heat source obliquely moving in an infinitely large conducting medium as in Fig. 5 (used by Hahn). The band heat source oA is infinitely long with a finite width $\overline{oA}$ and has an intensity of heat liberation of q_{pl} (in J/cm^2 s). Considering the band heat source oA as a combination of numerous infinitesimally small differential segments $\mathrm{d}l_i$, each of which is considered as an infinitely long moving line heat source, the temperature rise at any point $M(X,z)$ caused by any one of those segments, [using Eq. (3)], is given by

$$\theta_M = \frac{q_{pl}\,\mathrm{d}l_i}{2\pi\lambda} \mathrm{e}^{-(X - l_i \sin\varphi)V/2a} K_0\left[\frac{V}{2a}\sqrt{(X - l_i\sin\varphi)^2 + (z - l_i\cos\varphi)^2}\right].$$

Since the heat liberation intensity for the differential segmental heat source is q_{pl}, the heat liberation intensity for the line heat source is $q_{pl}\,\mathrm{d}l_i$. The distance between the line heat source and point M is $\sqrt{(X - l_i\sin\varphi)^2} + (z - l_i\cos\varphi)^2$, and its projection on the X-axis (i.e., direction of motion) is $(X - l_i\sin\varphi)$.

Thus the temperature rise at any point M caused by the entire oblique moving band heat source is given by

$$\theta_M = \frac{q_{pl}}{2\pi\lambda}\int_{l_i=0}^{L} \mathrm{e}^{-(X - l_i\sin\varphi)V/2a} \cdot K_0\left[\frac{V}{2a}\sqrt{(X - l_i\sin\varphi)^2}\bigcup(z - l_i\cos\varphi)^2\right]\mathrm{d}l_i. \tag{10}$$

Let

$$\frac{V}{2a}(X - l_i \sin\varphi) = u, \quad X - l_i \sin\varphi = \frac{2au}{V}, \quad l_i = \left(X - \frac{2au}{V}\right)\Big/ \sin\varphi, \quad \mathrm{d}l_i = -\frac{2a}{V\sin\varphi}\,\mathrm{d}u$$

when $l_i = 0$, $u = VX/2a$; and when $l_i = L$, $u = V(X - L\sin\varphi)/2a$.

Thus

$$\theta_M = \frac{q_{pl}}{\pi\lambda}\frac{a}{V\sin\varphi}\int_{u=V/2a(X-L\sin\varphi)}^{VX/2a} \mathrm{e}^{-u}\cdot K_0\left[\sqrt{u^2 + \frac{V^2}{4a^2}\left(z - \frac{X - 2au/V}{\tan\varphi}\right)^2}\right]\mathrm{d}u. \tag{11}$$

The non-dimensional temperature rise is given by

$$\frac{\pi\theta_M\lambda V}{aq_{pl}} = \frac{1}{\sin\varphi}\int_{u=V/2a(X-L\sin\varphi)}^{VX/2a} \mathrm{e}^{-u}\cdot K_0\left[\sqrt{u^2 + \frac{V^2}{4a^2}\left(z - \frac{X - 2au/V}{\tan\varphi}\right)^2}\right]\mathrm{d}u. \tag{12}$$

Since, in the derivation of Eqs. (11) and (12), a different coordinate system is used than Hahn's [Fig. 5], the non-dimensional temperature rise distributions on the band heat sources for various oblique angles (oblique angle φ is 80°, 60°, and 40°) were calculated and plotted [Fig. 8(a)–(c)]. A comparison of these results [Fig. 8(a)–(c)] with Hahn's [Figs. 3–5 of Ref. [11]) show that they are essentially the same. This confirms that Eqs. (11) and (12) presented here and Hahn's equations are essentially the same but expressed in different forms due to the use of different coordinate systems.

Fig. 8(a) shows the non-dimensional temperature rise distribution on the band heat source where the oblique angle φ is 80°. For this case, the angle between the plane of the band heat source and the direction of motion is 10° (refer to Fig. 5). It is also very close to Jaeger's model [10] where the direction of motion is parallel to the plane of the band heat source. Hence, the non-dimensional temperature rise distributions shown in Fig. 8(a) have essentially the same form as Jaeger's model, typically characterized by non-uniform distribution with the maximum towards the rear edge of the heat source. Fig. 8(c) shows the non-dimensional temperature rise distribution on the band heat source where the oblique angle φ is 40°. For this case, the angle between the plane of the band heat source and the direction of motion is 50° (refer to Fig. 5). It is to a certain extent close to Rosenthal's moving plane heat source model [8] (i.e., 50° instead of 90°) where the direction of motion is perpendicular to the plane of an infinitely large plane heat source. So, the non-dimensional temperature rise distributions shown in Fig. 8(c) have the form close to that of Rosenthal's model, typically characterized by uniform distribution over the heat source. As the heat source is an infinitely long band heat source with a finite width, near the edges the temperature rise would be lower than in the middle of the heat source. Thus, the equation for an infinitely large plane heat source moving in the direction perpendicular to the plane of the heat source in an infinite medium [8] and the equation for an infinitely long band heat source moving in the direction parallel to the plane of the heat source in an infinite medium [10] are two special cases of Hahn's general solution of an oblique moving plane heat source where the oblique angle φ is equals to 0° or 90°, respectively (see Fig. 9). Fig. 8(b) shows a situation in between Jaeger's [Fig. 8(a)] and Rosenthal's [Fig. 8(c)] models.

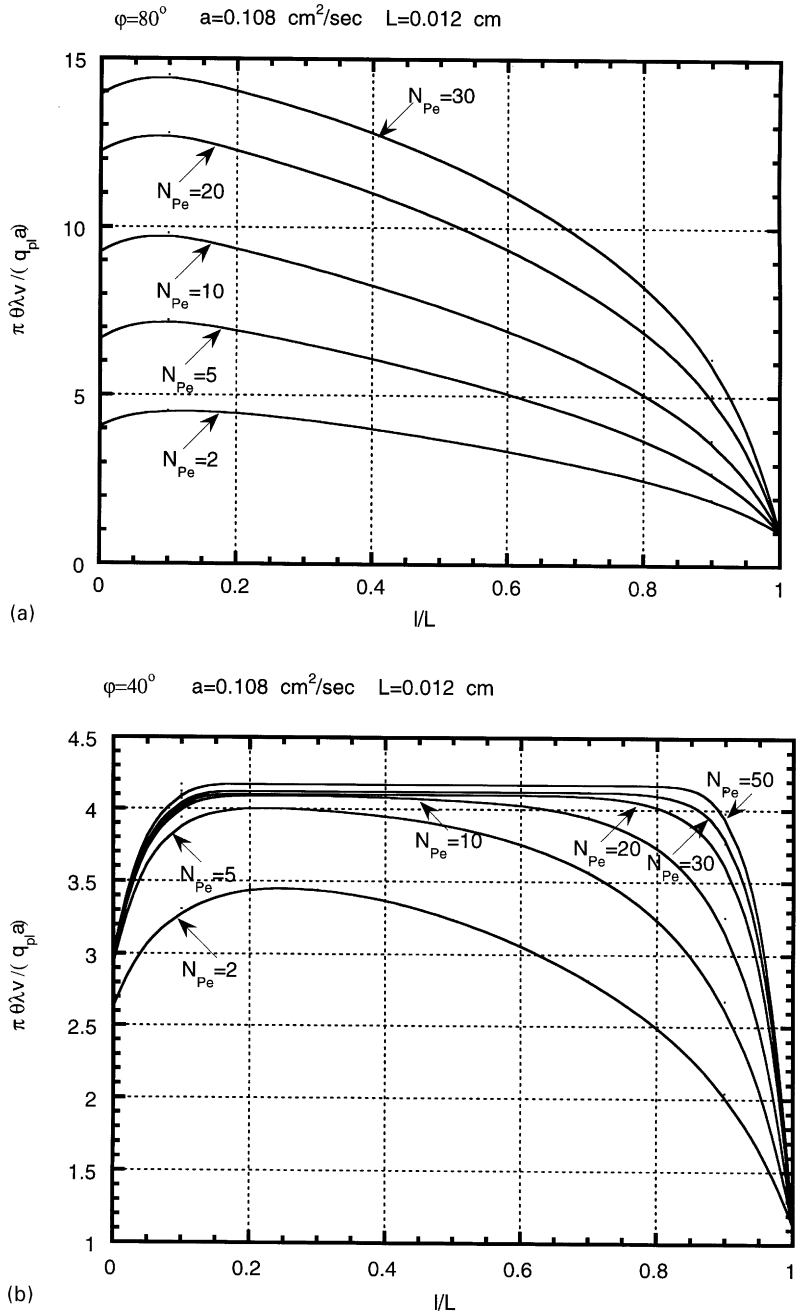

Fig. 8. Variation of the non-dimensional temperature rise along the band heat source moving obliquely in an infinite medium for various oblique angles and Peclet numbers.

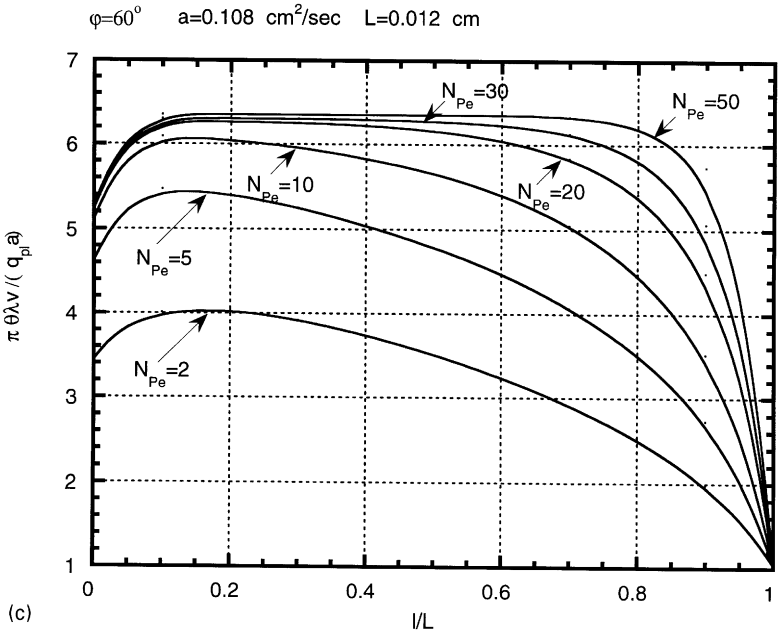

Fig. 8. (*Continued*).

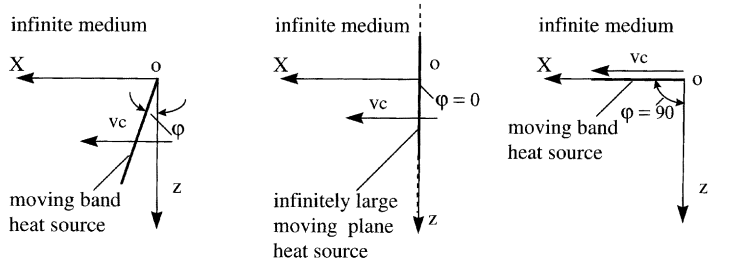

(a) Hahn's model for oblique moving band heat source

(b) Rosenthal's model for infinitely large moving band heat source

(c) Jaeger's moving band heat source model

Fig. 9. Comparison of Hahn's model with Rosenthal's and Jaeger's models.

3.3. Solution for a moving band heat source moving obliquely in a semi-infinite medium

For continuous chip formation in orthogonal machining, the shear plane heat source is moving in a semi-infinite medium with the work surface and the chip surface being the boundaries of a semi-infinite media. Thus, Hahn's oblique moving heat source solution should be modified with consideration for the effect of the boundaries and the use of appropriate image sources.

Fig. 10 is a schematic of a band heat source moving obliquely at an angle φ in a semi-infinite medium. The upper boundary of the semi-infinite body can be considered adiabatic for many

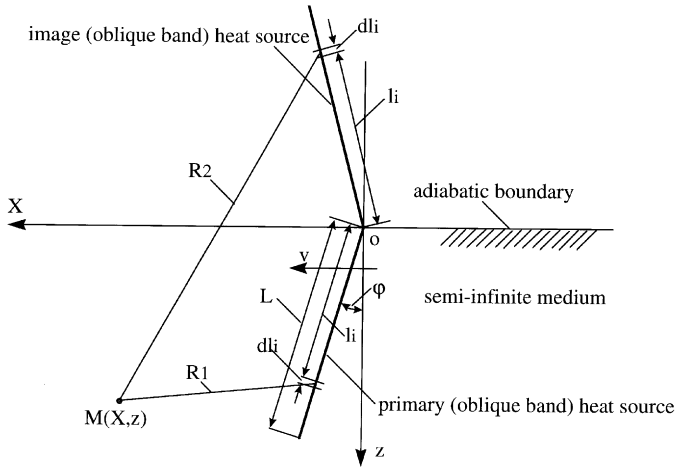

Fig. 10. Schematic of the modified Hahn's model for an oblique moving band heat source in a semi-infinite medium.

practical cases involving machining dry, i.e., without enhanced cooling. For an adiabatic boundary, an image heat source (a mirror image of the primary heat source with respect to the boundary surface) with the same heat liberation intensity should be considered as shown in the figure. A moving coordinate system is used for the analysis of the thermal effect caused by the oblique moving band heat source, where oX is the abscissa and oz is the ordinate of the system. The origin of the system coincides with the upper end of the oblique moving band heat source and moves together with it with the same velocity and in the same direction.

The temperature rise at any point $M(X, z)$ is due to the combined effect of the primary and the image heat sources. Each of these heat sources can be considered as a combination of numerous infinitesimal segments $\mathrm{d}l_i$, with each again as an infinitely long moving line heat source. Thus, the temperature rise at any point M caused by the segmental moving line heat source $\mathrm{d}l_i$ can be calculated using Eq. (3). For any one of the segmental moving line heat source $\mathrm{d}l_i$ (see Fig. 10): $q_l = q_{pl}\,\mathrm{d}l_i$; the distance between point M and the primary segmental line heat source, R_1, is $\sqrt{(X - l_i \sin\varphi)^2 + (z - l_i \cos\varphi)^2}$; the distance between point M and the image source, R_2, is $\sqrt{(X - l_i \sin\varphi)^2 + (z + l_i \cos\varphi)^2}$; and the projection of these distances on the X-axis (direction of the motion) is $(X - l_i \sin\varphi)$.

Thus, the temperature rise at any point M caused by a segmental moving line heat source $\mathrm{d}l_i$ including its image heat source is given by

$$\mathrm{d}\theta_M = \frac{q_{pl}\,\mathrm{d}l_i}{2\pi\lambda} \mathrm{e}^{-(X - l_i \sin\varphi)V/2a} \left\{ K_0 \left[\frac{V}{2a} \sqrt{(X - l_i \sin\varphi)^2 + (z - l_i \cos\varphi)^2} \right] + K_0 \left[\frac{V}{2a} \sqrt{(X - l_i \sin\varphi)^2 + (z + l_i \cos\varphi)^2} \right] \right\}. \tag{13}$$

The total temperature rise at any point M caused by the complete oblique moving band heat source including its image heat source of equal intensity is given by

$$\theta_M = \frac{q_{pl}}{2\pi\lambda}\int_{l_i=0}^{L} e^{-(X-l_i\sin\varphi)V/2a}\left\{K_0\left[\frac{V}{2a}\sqrt{(X-l_i\sin\varphi)^2+(z-l_i\cos\varphi)^2}\right] + K_0\left[\frac{V}{2a}\sqrt{(X-l_i\sin\varphi)^2+(z+l^i\cos\varphi)^2}\right]\right\}dl_i. \quad (14)$$

The non-dimensional temperature rise at any point M caused by the entire oblique moving band shear plane heat source including its image heat source is given by

$$\frac{\theta_M\lambda}{q_{pl}L} = \frac{1}{2\pi L}\int_{l_i=0}^{L} e^{-(X-l_i\sin\varphi)V/2a}\left\{K_0\left[\frac{V}{2a}\sqrt{(X-l_i\sin\varphi)^2+(z-l_i\cos\varphi)^2}\right] + K_0\left[\frac{V}{2a}\sqrt{(X-l_i\sin\varphi)^2+(z+l_i\cos\varphi)^2}\right]\right\}dl_i. \quad (15)$$

The first term in the brackets is due to the shear plane heat source and the second term is due to its image heat source.

4. Results of thermal model computations

To compute the temperature distribution in the workmaterial and the chip due to the shear plane heat source using the exact analysis developed in this investigation, experimental data from Loewen and Shaw [14] (Table 2) is considered first. This is followed by the use of additional experimental data of other researchers [13,17,32] presented under "Discussion" to compare the results for two different steels, conventional machining versus ultraprecision machining, and the effect of thermal number.

Table 2
Cutting data for machining steel from Loewen and Shaw [14]

Work material	SAE B1113 steel
Tool	K2S carbide 20° rake, 5° clearance angle
Type of cut	Orthogonal
Cutting speed	$V_c = 139$ m/min (232 cm/s)
Undeformed chip thickness	$t = 0.006$ cm
Width of cut	$w = 0.384$ cm
Chip contact length	$L_c = 0.023$ cm
Cutting force	$F_c = 356$ N
Feed force	$F_t = 125$ N
Chip thickness ratio	$r = 0.51$
Thermal diffusivity	$a = 0.1484$ cm^2/s
Thermal conductivity	$\lambda = 0.567$ J/cm s °C

For applying Eq. (14), the following parameters, namely, the shear angle ϕ, the shear force F_s, the shear velocity V_s, the length of shear plane L, the heat liberation intensity of the shear band heat source q_{pl}, and the chip flow velocity V_{ch} were calculated using the classical orthogonal metal cutting theory [30,31,33] and data from Table 2 [31]:

$$\phi = 30.1^\circ, \quad F_s = 245.3 \text{ N}, \quad V_s = 221.4 \text{ cm/s},$$

$$L = 0.01196 \text{ cm}, \quad q_{pl} = 118253 \text{ J/cm}^2\text{s}, \quad V_{ch} = 118.18 \text{ cm/s}.$$

Substituting in Eq. (14) the relevant parameters and the data obtained above, the temperature rise at various points in the chip near the shear plane can be computed. In this investigation a Gateway Personal Computer (200 MHz) is used. The computational speed using a simple program is fairly high (about 300 points/min).

4.1. Temperature rise distribution in the workmaterial due to the shear plane heat source

For calculating the temperature rise in the workmaterial near the shear band heat source, the heat transfer model shown schematically in Fig. 6(a′) is used. The area concerned is that under the line **aoe** (from $X = 50$ μm to $X = -250$ μm and $z = 0$ μm to $z = 150$ μm). In this example, this area is divided into 30×20 elements; thus the number of nodes is 651. Using Eq. (14), where the oblique angle φ is $-(90 - \phi)$ [see Fig. 6(a′)], the temperature rise at each node in the workmaterial near the shear plane is calculated. It may be noted that the computational accuracy is independent of the number of elements and nodes in the area concerned because Eq. (14) is an exact analytical solution of the band heat source moving obliquely in a semi-infinite medium. This is the main advantage of the heat source method over the finite element or finite difference methods used by other researchers [20,25]. Based on this data and using the principle of interpolation, isotherms of the temperature rise are plotted as shown in Fig. 11(a). They are based on the model shown in Fig. 6(a′) where the part of the material on the right of the heat source, i.e., part **oedc** shown in Fig. 6(a′) is imaginary and an extension. Its real form and location are shown as Part II in the same schematic. Thus, the temperature rise distribution (in the form of a series of isotherms) obtained in the imaginary part of Fig. 6(a′) cannot be used and only the distribution picture in front of and beneath the shear band heat source [i.e. in the workmaterial side in Fig. 11(a)] is used. For the temperature rise distribution in the chip (Part II) due to the shear plane heat source, it is necessary to solve the equation separately, using the model shown in Fig. 6(b′).

4.2. Temperature rise distribution in the chip due to the shear plane heat source

For calculating the distribution of the temperature rise in the chip due to the shear band heat source, the heat transfer model shown in Fig. 6(b′) is used. The area covered is that under the chip boundary line **aoe** (from $X = 50$ μm to $X = -150$ μm and $z = 0$ μm to $z = 150$ μm). In this example, this area is divided into 20×15 elements; thus the number of nodes is 236. Using Eq. (14), where the oblique angle φ is $(\phi - \alpha)$, [see Fig. 6(b′)], the temperature rise at each node is calculated. Using the principle of interpolation, the isotherms of various temperature are plotted [Fig. 11(b)].

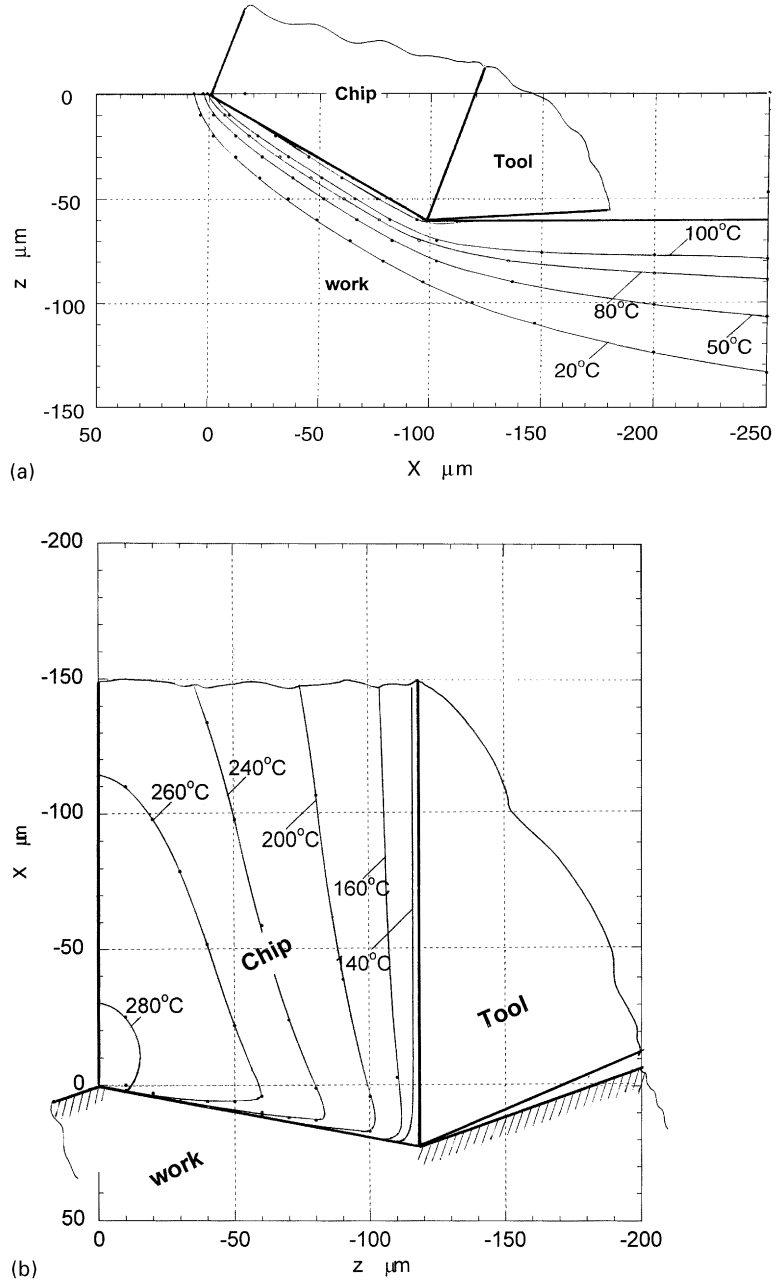

Fig. 11. (a) Temperature rise distribution in the workmaterial during machining of SAE B1113 steel due to shear plane heat source, using modified Hahn's model and data from Shaw [31]; (b) Temperature rise distribution in the chip during machining of SAE B1113 steel due to shear plane heat source, using modified Hahn's model and data from Shaw [31]; (c) Temperature rise distribution in the chip and workmaterial during machining of SAE B1113 steel due to shear plane heat source, using modified Hahn's model and data from Shaw [31]).

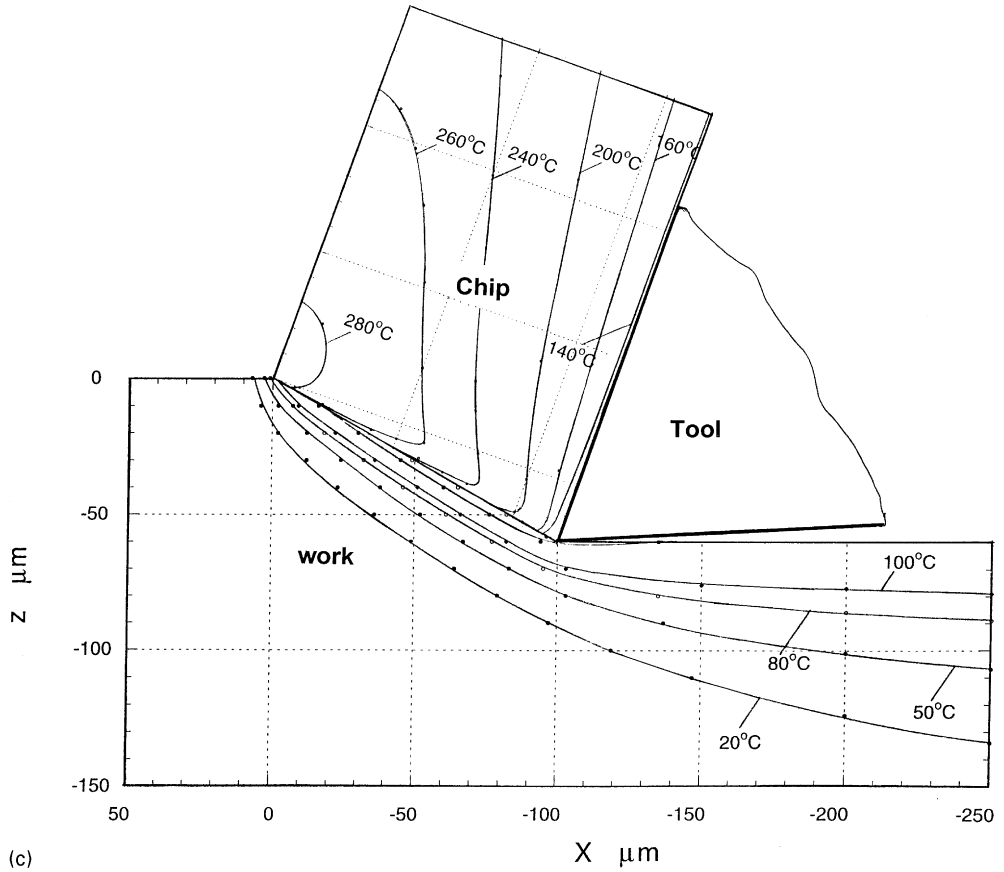

Fig. 11. (*Continued*).

They are calculated based on the model shown in Fig. 6(b′) where the part of the material under the heat source, part **oedc** shown in Fig. 6(b′), is an extension into the workmaterial. Its real form and location are shown as Part I in the same schematic. Thus the temperature rise distribution obtained in the imaginary part of Fig. 6(b′) is not used, instead the temperature field calculated in Part II (chip side) is used directly.

4.3. Temperature rise distribution in machining due to shear plane heat source only

Using the data of the temperature rise on the chip side [used in plotting Fig. 11(b)] within the length of the chip–tool contact, the average temperature rise in the chip volume, $\bar{\theta}_s$ caused by the main shear plane heat source is calculated as 204.7° and the chip–tool interface temperature, $\bar{\theta}_{chip-tool}$ as 130° (see Table 3) for conventional machining of steel (SAE B 1113). Fig. 11(c) shows the isotherms of the temperature rise distribution in the work and the chip obtained by combining the

Table 3
Workmaterial-AISI 1113 steel (Shaw [31]) (cutting data: $\alpha = 20^\circ$, $v_c = 2.32$ m/s, $t_c = 0.006$ cm, $w = 0.384$ cm, $F_c = 356$ N, $F_t = 125$ N, $r = 0.51$, $\lambda = 0.567$ J/cm s °C, $a = 0.1484$ cm^2/s, $N_{th} = 9.38$)

	Trigger and Chao's method	Boothroyd's method	Loewen and Shaw's method	Leone's method	Exact analysis (Modified Hahn's model)
B	0.1	0.18	0.375	0.3617	[a]
$1 - B$	0.9	0.82	0.625	0.6383	[b]
$\bar{\theta}_s$	197.4	218.1	166.2	169.8	204.7
$\bar{\theta}_{chip-tool}$	197.4	218.1	166.2	169.8	130

[a] $B_{appr} = 0.2304$.
[b] $(1 - B_{appr}) = 0.7696$.

temperature distribution in the workmaterial from the first model and the temperature distribution in the chip from the second model [Figs. 11(a) and (b)].

5. Discussion

5.1. On the assumption of a shear plane instead of a shear zone

In Fig. 11(c), a sudden change in the temperature rise on either side of the shear band heat source can be seen. For example, on the workmaterial side, the temperature near the shear zone is $\sim 140^\circ$C but the temperature near the shear zone on the chip side varies considerably from $\sim 140^\circ$C near the tool tip to $\sim 280^\circ$C near the intersection of the chip and the workmaterial. This is because the shear plane is assumed as a line instead of a zone. In practice, the shear band has a finite thickness, albeit small. The changes in the heat transfer conditions take place continuously and gradually, such as the velocity of the moving heat source from V_c at the workmaterial side to V_{ch} at the chip side in this shear zone. Hence, no discontinuity in the temperature rise distribution should be present. In this investigation, the heat transfer model considered for the temperature rise distribution on the workmaterial side uses an oblique moving heat source moving with the cutting velocity at an oblique angle of $\varphi = -(90 - \phi)$ while on the chip side uses an oblique moving heat source moving with the chip velocity at an oblique angle of $\varphi = -(\phi - \alpha)$. The transition between them is not considered as shear is assumed to be localized in a single plane instead of a zone.

Thus, in metal cutting, there is a transient heat transfer process taking place together with the material flow as the material passes from the workmaterial to the chip via an extremely thin shear zone. As a result, on either side of the shear zone (outside of the shear band heat source of certain thickness), a rather noticeable difference in the temperature rise can be noted. The transient processes occurring in the small thickness of the shear band heat source are usually not considered. In fact, the difference in the temperature on either side of the shear band is a result of the gradual and continuous changes taking place in the shear zone of finite thickness. Hence, the consideration of matching temperatures of either side of the shear zone, which is necessary for solutions based on heat partition, is neither necessary nor correct.

5.2. On the uniform temperature rise distribution in the chip and the workmaterial due to shear plane heat source

Consideration of uniform temperature rise distribution in the material passing through the heat source, which is an assumption made in many of the approximate methods, is true only for the case where the heat source is infinitely large and moving in an infinite medium. The solution for this case is given by Rosenthal [8] [refer to Fig. 9(b)]:

When $X > 0$ (i.e., before entering the heat source)

$$\theta = \frac{q_{pl}}{c\rho v} e^{-Xv/a}. \tag{16}$$

When $X \leqslant 0$ (i.e., after passing through the heat source)

$$\theta = \frac{q_{pl}}{c\rho v}. \tag{17}$$

It can be seen from Eq. (17) that for the case shown in Fig. 9(b), the temperature rise at any point in the conducting medium passing through the heat source is constant and independent of the location of the point. That means in the infinite medium which has passed through an infinitely large plane heat source, the temperature rise distribution is uniform and the temperature rise is the same everywhere. This is also true for its equivalent case shown in Fig. 12, i.e., a bar of finite cross-section with adiabatic boundaries (i.e., no heat loss across its sides) passing through a uniform heat source. In part of the bar passing through the heat source, the distribution of the temperature rise is uniform, as expressed by Eq. (17). But this is not the case in metal cutting. Because all the four boundaries of the chip during orthogonal metal cutting can never be all adiabatic. Thus, in the chip, passing through the shear plane heat source of finite size, the distribution of the temperature rise can not be uniform even though the heat liberation intensity is uniform over the heat source. Thus, the assumption of uniform distribution of temperature rise in the chip and use of approximate equation [Eq. (1)] can lead to erroneous results.

The distribution of temperature rise in the chip near the shear band heat source is shown in Figs. 11(b) and (c). They show that the temperature rise along the chip–tool interface is $\sim 130^{\circ}$C,

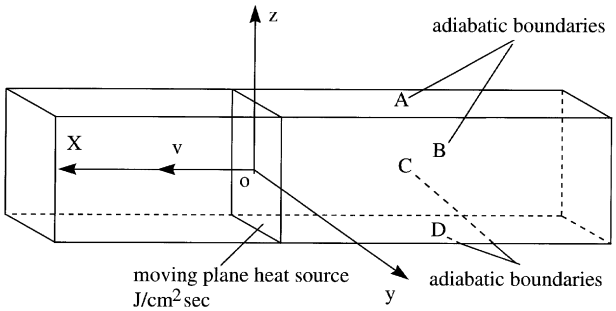

Fig. 12. Schematic of a model equivalent to the Rosenthal's model, as shown in Fig. 9(b).

and on its adiabatic boundary (i.e., on the upper surface of the chip) in the range of $\sim$ 230–300°C. From this, it is clear that the temperature distribution is non-uniform. Within the range of the length of the chip–tool contact, the average temperature rise of the whole chip volume $\bar{\theta}_s$ is found to be $\sim$ 205°C. By considering the average temperature rise of the whole volume of the chip ($\sim$ 205°C) as the average temperature rise on the chip–tool interface (130°C), significant error (50% or larger) can result.

5.3. Comparison of various thermal models used for the shear plane heat source

Since we are considering the temperature distribution in the workmaterial and the chip near the shear plane due to one heat source only, namely, the shear plane heat source, instead of considering the combined effect of shear plane heat source and the frictional heat source at the chip–tool interface, it would not be possible to compare the results of exact analysis with experimental values directly. However, it is possible to compare the results obtained by various methods, some of which were compared with experiments. Thus the validity of the exact analysis can be determined somewhat indirectly.

Hahn's modified solution presented here is the general case, while Rosenthal's [8] (for the case of moving velocity *perpendicular* to the moving heat source) and Jaeger's [10] (for the case of moving velocity *parallel* to the moving heat source) solutions are special cases. These are exact solutions based on the real nature of the moving plane heat source problems with minimal simplifications and/or assumptions. Consequently, they are expected to yield more accurate results. For a comparison of various methods, the heat partition fractions for the chip and the workmaterial, the average temperature rise in the chip, and the average temperature rise at the chip–tool interface are calculated for the same example but using different models. Table 3, summarizes the results based on Shaw's data [31].

In utilizing Hahn's solution, one avoids making an explicit *a priori* assumption regarding partitioning of heat between the workmaterial and the chip, as was common in most prior work. Instead, this information is provided as part of the solution. Using the average temperature rise in the chip, the fraction of the heat energy going into the chip can be calculated (see Table 3). Thus the real partition fraction of the heat liberated from the shear zone heat source can be evaluated and compared with the values used in the various models considered here. The partition fraction, obtained in this way, includes all the heat, namely, by conduction and that due to the heat energy flow due to material flow. In this paper, this heat partition is termed as the apparent heat partition fraction, and it is designated as B_{appr} for the workmaterial and $(1 - B_{appr})$ for the chip.

The values of heat partition for the chip $(1 - B)$ (see Table 3) are lower by Loewen and Shaw's (0.625) and Leone's (0.6383) methods and higher by Boothroyd's (0.82) and Trigger and Chao's [13] (0.9) methods than by exact method (0.7696). Thus the actual values of the average temperature rise in the chip, $\bar{\theta}_s$, caused by the shear zone heat source would be higher than that obtained by Loewen and Shaw's and Leone's methods; lower than that obtained by the Boothroyd's method when the thermal number N_{th} is high ($N_{th} > 8$); and close to Trigger and Chao's method for conventional machining of steel. Table 3 also gives the average temperature rise ($\bar{\theta}_s$) in the chip calculated by various methods. The exact analysis gives a value of 204.7°C which is higher than Loewen and Shaw's (166.2°C) and Leone's (169.8° C) models, and lower than Boothroyd's method (218.0° C), and close to Trigger and Chao's method (197.4° C). As Trigger and Chao used conditions closer to

practice and since their values were closer to the values obtained by the exact analysis, it may be inferred that the exact analysis yields results closer to practice.

For further consideration of the model, including a comparison of conventional versus ultraprecision machining, i.e., ultraprecision machining of aluminum with a diamond tool versus conventional machining of steel with a carbide tool, comparison of two different steels, and the effect of thermal number, additional metal cutting data available in the literature was used for comparison. Tables 4–6 give the results of the calculations of three metal cutting examples. Table 4 (data from Boothroyd [30]) and Table 5 (data from Trigger and Chao [13]) are for two types of steel, and Table 6 (data from Ueda et al. [32]) is for ultraprecision machining of aluminum using a single crystal diamond. It can be seen that Tables 4 and 5 yield the same conclusions as in the first example (Table 3). For example, the assumed fraction of heat into the workmaterial, in general, is lower by Trigger and Chao's [13] and Boothroyd's [30] methods and higher by Loewen and Shaw's [14] and Leone's [15] methods than that obtained by the exact analysis.

It can be shown that for ultraprecision machining of aluminum [32] (see Table 6), the thermal number is low (0.935) due to high thermal conductivity of aluminum and very low feed rate. It can be seen from Fig. 3, that for low values of N_{th}, i.e., $N_{th} \tan \phi < 1$, Boothroyd's method yields values

Table 4
Workmaterial-mild steel (Boothroyd [30]) (cutting data: $\alpha = 0^\circ$, $v = 2$ m/s, $t_c = 0.025$ cm, $w = 0.25$ cm, $F_c = 890$ N, $F_t = 667$ N, $r = 0.3$, $\lambda = 0.436$ J/cm s °C, $a = 0.1206$ cm^2/s, $N_{th} = 41.46$)

	Trigger and Chao's method	Boothroyd's method	Loewen and Shaw's method	Leone's method	Exact analysis (Modified Hahn's model)
B	0.1	0.1	0.2822	0.2578	[a]
$1 - B$	0.9	0.9	0.7178	0.7422	[b]
$\bar{\theta}_s$	232.8	275.0	219.0	226.7	258
$\bar{\theta}_{chip-tool}$	232.8	275.0	219.0	226.7	145.3

[a] $B_{appr} = 0.1553$.
[b] $(1 - B_{appr}) = 0.8447$.

Table 5
Workmaterial-Ne 9445 (Trigger and Chao [13]) (cutting data: $\alpha = 4^\circ$, $v = 1.524$ m/s., $t_c = 0.02489$ cm, $w = 0.2591$ cm, $F_c = 1681.3$ N, $F_t = 854.0$ N, $r = 0.375$, $\lambda = 0.3888$ J/cm s °C, $a = 0.0955$ cm^2/s, $N_{th} = 39.72$)

	Trigger and Chao's method	Boothroyd's method	Loewen and Shaw's method	Leone's method	Exact analysis (Modified Hahn's model)
B	0.1	0.08	0.2646	0.2407	[a]
$1 - B$	0.9	0.92	0.7354	0.7593	[b]
$\bar{\theta}_s$	383.2	461.8	369.2	381.1	420.2
$\bar{\theta}_{chip-tool}$	383.2	461.8	369.2	381.1	240.8

[a] $B_{appr} = 0.1629$.
[b] $(1 - B_{appr}) = 0.8371$.

Table 6
Workmaterial-Aluminum (Ueda et al. [32]) (cutting data: $\alpha = -5^\circ$, $v = 8.63$ m/s, $t_c = 0.001$ cm, $w = 0.1$ cm, $F_c = 12.4$ N, $F_t = 8.1$ N; $r = 0.2853$, $\lambda = 2.368$ J/cm s °C, $a = 0.9232$ cm^2/s, $N_{th} = 0.935$)

	Trigger and Chao's method	Boothroyd's method	Loewen and Shaw's method	Leones method	Exact analysis (Modified Hahn's model)
B	0.1	≈ 0.70	0.7327	0.7011	[a]
$1 - B$	0.9	≈ 0.30	0.2673	0.2989	[b]
$\bar{\theta}_s$	312.7	121.0	107.8	120.6	140.6
$\bar{\theta}_{chip-tool}$	312.7	121.0	107.8	120.6	133

[a] $B_{appr} = 0.6514$.
[b] $(1 - B_{appr}) = 0.3486$.

of heat partition fraction for the chip closer to the experimental values. Consequently, the value of the average temperature rise in the chip should also be closer to the experimental values. The value of the heat partition into the chip by Boothroyd's method is 0.3 and that by the exact method is 0.3486. The average temperature rise in the chip calculated by Loewen and Shaw's and Leone's methods are 107.8°C and 120.6°C, respectively and that by Boothroyd's method is 121.0°C. Trigger and Chao's method yields far higher temperature, namely, 312.7°C because of the higher heat partition fraction assumed for this case. The average temperature rise in the chip calculated by the exact analysis is 140.6°C. It can be seen that the temperature calculated by the exact analysis is much closer to that calculated by Boothroyd's method for low thermal numbers.

Using the exact analysis, the temperature rise at the chip–tool interface caused by the shear plane heat source for ultraprecision machining of aluminum using a single crystal diamond [32] is found to be 133°C. Using the analytical solutions for the frictional heat source at the chip–tool interface (shown in Part II) [26], the average temperature rise on the chip–tool interface caused by the frictional heat source was found to be ≈ 20°C. Assuming the room temperature at 20°C, the total temperature at the chip–tool interface is 173°C. Ueda et al. reported an experimental value of 171°C showing the calculated results using the exact analysis are close to the actual values in ultraprecision machining of aluminum.

5.4. *Comparison of Trigger and Chao* [13] *and Boothroyd* [17] *methods*

It can be seen from Tables 3–5, the values of B obtained by Trigger and Chao's [13] and Boothroyd's [17] methods are close (generally Trigger and Chao's B are higher than Boothroyd's) especially for machining steels but the values of $\bar{\theta}_s$ are quite different. This is because Trigger and Chao's method yields lower value for $\bar{\theta}_s$ as they consider only $\sim 87.5\%$ of the energy of deformation in the shear band is available as sensible heat.

5.5. *On the non-uniformity in the temperature distribution*

Using Eq. (14), the temperature rise distributions in the chip [for the examples given in Tables 4–6] are shown in Figs. 13(a)–(c). From these figures as well as from Fig. 11(b), the

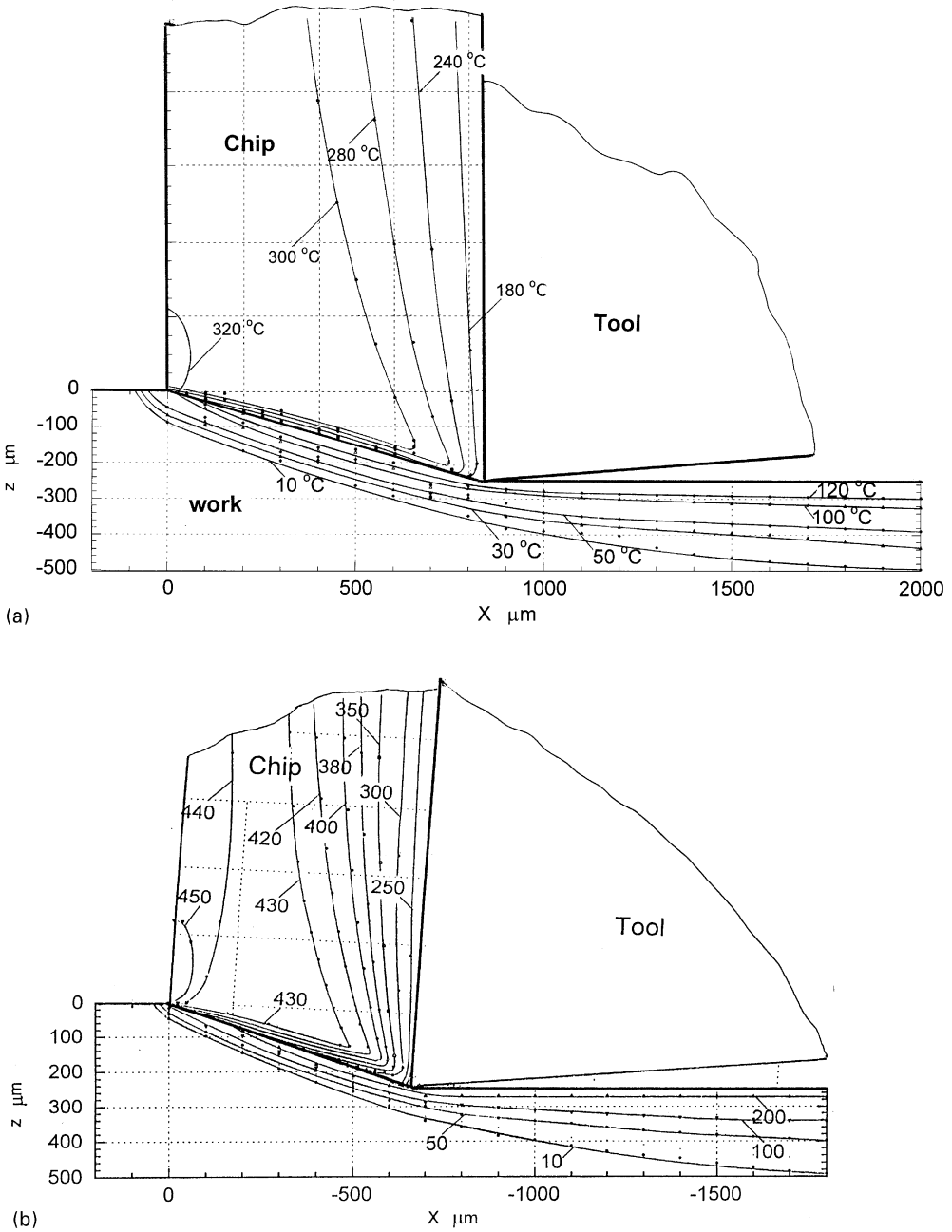

Fig. 13. (a) Temperature rise distribution in the workmaterial and chip during machining of mild steel due to shear plane heat source, using modified Hahn's model (data from Boothroyd [30]); (b) Temperature rise distribution in the workmaterial and chip during machining of NE 9445 steel due to shear plane heat source, using modified Hahn's model (data from Trigger and Chao [13]); (c) Temperature rise distribution in the workmaterial and chip during machining of aluminum due to shear plane heat source, using modified Hahn's model (data from Ueda et al. [32]).

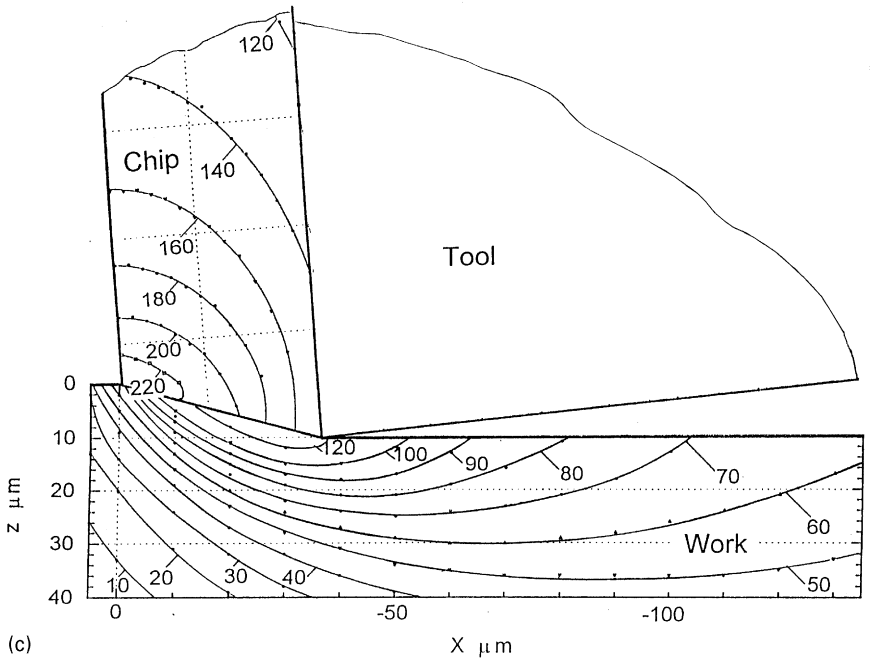

Fig. 13. (*Continued*).

non-uniformity in the temperature distributions of the chip within the range of chip–tool contact length can be seen to be significant. It can also be seen that the temperature of the chip is much higher in Fig. 13(b) than Fig. 13(a) due to differences in the nature of the workmaterial and consequent cutting forces (see Tables 4 and 5). Also, a comparison of Figs. 13(b) and (c) show that the temperature contours near the shear plane on the workmaterial side are closer (i.e. temperature gradient higher) in the case of steel (Table 5) than aluminum (Table 6). This is attributed to the high thermal conductivity and consequent lower thermal number in the case of aluminum.

From Figs. 11(b) and 13(a)–(c), the non-uniformity of the temperature rise distribution along the chip thickness direction can also be seen to be quite significant for the cases considered in this investigation. Thus, the average temperature rise in the chip $\bar{\theta}_s$ can not be considered as the average temperature rise at the chip–tool contact interface $\bar{\theta}_{chip-tool}$. The difference between $\bar{\theta}_s$ and $\bar{\theta}_{chip-tool}$ can be significant (see the values given in Tables 4–6 using the exact solution of the oblique moving band heat source).

5.6. Effect of thermal number on the temperature distribution at/or near the shear plane and chip–tool interface

In 1953, Chao and Trigger [12] in an important paper on, "The Significance of the Thermal Number in Metal Cutting," came to the conclusion that the temperature distribution along the shear plane (i.e. the heat partition fraction) is solely dependent on the thermal number ($v_c t/k$). They

demonstrated this by varying the cutting velocity and the uncut chip thickness in machining of an SAE 52100 steel workmaterial with a triple carbide tool. For example, they showed a parabolic increase in the shear angle and a corresponding decrease in the specific work done in cutting with increase in thermal number, N_{th}. Unfortunately, since they examined only one workmaterial, they could not vary the thermal diffusivity parameter which is in the denominator of the thermal number, N_{th}. Hahn [34], in a discussion to Chao and Trigger's work [12] pointed out that because thermal diffiusivity is not varied, the plots of the variation of shear angle with thermal number do not prove that the shear angle is related to the thermal number but only to the product of the cutting speed and depth of cut (i.e., removal rate).

In this investigation, we have examined the effect of heat partition on a range of thermal numbers, N_{th} from a low of 0.935 to a high of 41.46 (see Tables 3–6) based on the experimental results published in the literature [13,30–32]. This includes different cutting velocities (1.524–8.63 m/s), depths of cut (0.001–0.025 cm), and thermal diffusivities (0.1206–0.9232 cm^2/s for four different workmaterials (three different steels namely, (AISI 1113 [30], mild steel [30], and SAE 9445 [13], and, one aluminum [32]). Table 7 shows the relationship between the thermal number, N_{th} and the heat partition fraction, $B_{apparent}$ (see Tables 3–6 for details) obtained from the analytical

Table 7
Relationship between heat partition fraction in the workmaterial, $B_{apparent}$, and the thermal number, N_{th}, due to shear plane heat source

Thermal number, N_{th}	0.935	9.380	39.72	41.46
Heat partition, $B_{apparent}$	0.6514	0.2304	0.1629	0.1553

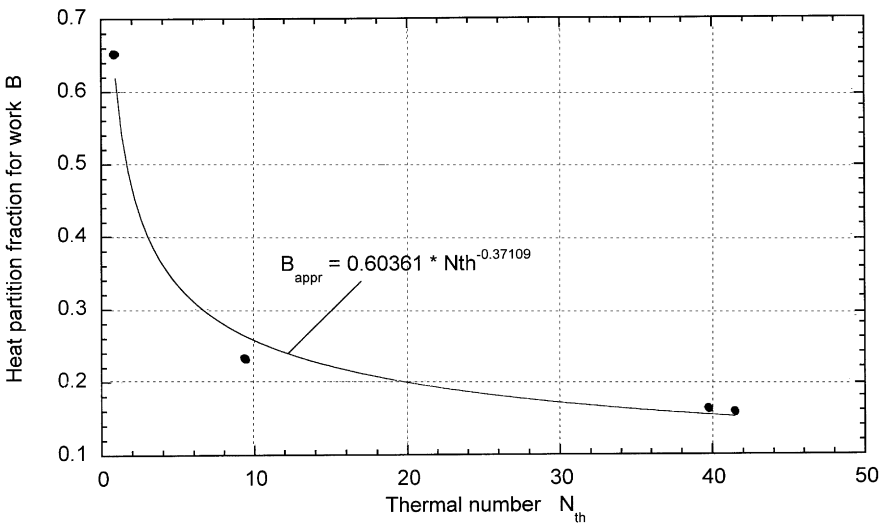

Fig. 14. Variation of the heat partition in the workmaterial, $B_{apparent}$, with the thermal number, N_{th}, due to shear plane heat source.

results obtained in this investigation. Fig. 14 shows the variation of the $B_{apparent}$ with the thermal number, N_{th}. It can be seen that with increase in the thermal number, the heat partition fraction decreases. The approximate relationship is of the form

$$B_{apparent} = 0.60361 \times N_{th}^{-0.37101}.$$

This relationship is found to be very similar to the results obtained by Chao and Trigger [12]. Since all the parameters in the thermal number are varied in this investigation, it reinforces the conclusion of Chao and Trigger [12], namely, the temperature distribution along the shear plane (i.e., the heat partition fraction) is solely dependent on the thermal number ($v_c t/k$). It will be shown in Part III [27] that this is so because of the minimal contribution from the frictional heat source.

Two other conclusions may be drawn from the relationship between the thermal number and the temperature distribution near the shear plane and the chip–tool interface due to the shear plane heat source. First, it can be seen from Figs. 11(a), 13(a) and (b) for cases where the thermal numbers are high ($N_{th} \approx$ 9–40), the high temperature isotherms near the shear plane in the workmaterial are concentrated within a very narrow zone ($\leqslant 0.2$ of the depth of cut). Beyond this ($\approx$ 0.3–05 of the depth of cut), the temperature rise approaches zero [Figs. 11(a), 13(a) and (b)]. But for low thermal numbers ($N_{th} \approx 0.9$) [32] because of low cutting speed and good thermal conductivity of the workmaterial this in not the case [see Fig. 13(c)]. Second, for cases where the thermal numbers are high ($N_{th} \approx$ 9–40) the temperature at the tool–chip interface, i.e., from the tool tip to the point where the chip leaves the tool face, the temperature is uniformly rather distributed [see Figs. 11(a), 13(a) and (b)]. But for low thermal numbers ($N_{th} \approx 0.9$) [32], the non-uniformity of the temperature distribution is quite significant [see Fig. 13(c)], i.e., it varies from $\approx$150°C at the tool tip to $\approx$ 100°C at the point where the chip leaves the tool rake face.

6. Conclusion

1. A new approach for the temperature distribution in the chip and the workmaterial near the shear plane due to shear plane heat source only is presented. The analysis is made in two separate parts, namely, the workmaterial side and the chip side of the shear plane and then combined. The workmaterial (or the chip) is extended past the shear plane as an imaginary region for continuity to determine the temperature distribution in the workmaterial (or the chip) near the shear plane. The imaginary regions are the regions either of the workmaterial that was cut by the cutting tool prior to this instance and became the chip or will be cut by the cutting tool prior to becoming the chip. An appropriate image heat source with the same intensity as the shear plane heat source is considered for each case. The temperature distributions in the chip and the workmaterial were determined separately by this method and combined to obtain isotherms of the total temperature distribution (and not merely the average temperatures).

2. The analytical solution presented here (based on Hahn's original model), for an obliquely moving band heat source in a semi-infinite medium with appropriate image sources is an exact

solution. For this solution, it is not necessary to make an explicit a priori assumption regarding heat partition between the chip and the workmaterial, as was common in earlier works. Instead, this information is provided as part of the solution.

3. The exact solution is closer to the real nature of the chip formation process in machining. It involves heat conduction as well as that due to heat carried by the material flow which is common in many moving heat source problems.

4. For a continuous chip formation process, the material on either side of the heat source (oblique moving shear plane heat source) is the same, i.e., the material of the chip is coming from the workmaterial side via the shear plane. The material of the chip and the workmaterial is therefore continuous. However, between them exists the shear plane heat source where both heat and mass transfer are involved. The heat transfer by conduction and by material transport occur simultaneously. Hence, the chip and the undeformed material in the workmaterial cannot be considered as two separate bodies in sliding contact.

5. From the point of view of heat transfer, the chip formation process at the shear plane in metal cutting is entirely different from the frictional sliding contact between two separate bodies. Hence, Blok's heat partition principle of matching temperatures on either side of the frictional heat source at the sliding contact would be unsuitable for the analysis of the temperature in the shear zone in machining as Blok himself indicated (see discussion of Ref. [14]).

6. It was shown that consideration of uniform distribution of temperature rise in the chip near the shear band heat source can lead to significant errors (as much as 50%).

7. The average temperature rise along the chip–tool interface is considerably lower than the average temperature rise in the chip volume near the shear band heat source. The consideration of equating the average temperature rise along the chip–tool interface and the average temperature rise in the whole chip volume near the shear band heat source is not correct.

8. Based on the analytical results presented here (Tables 3–6) it can be seen that the heat partition fraction into the workmaterial, B, due to the shear plane heat source varies with the thermal number. From this, it can be concluded that the temperature distribution along the shear plane (i.e. the heat partition fraction) is solely dependent on the thermal number, $N_{th}(v_c t/k)$, as Chao and Trigger [12] originally concluded. It may be noted that this was established in this investigation by varying all the parameters in the thermal number, namely, the cutting velocity, the depth of cut, and the thermal diffusivities of the workmaterial (three steels and one aluminum) from the experimental results published in the literature [13, 30–32]. It can also be concluded that the temperature isotherms in the workmaterial are concentrated near the shear plane for high thermal numbers ($N_{th} \approx 9.38$–41.46 [12,30,31]) while this is not the case for low thermal numbers ($N_{th} \approx 0.9$ [32]). Similarly, the temperature distribution is more uniform at the chip–tool interface for high thermal numbers but not for low thermal numbers.

9. The results presented here are for the temperature rise distribution in the chip and the workmaterial near the shear plane due to the shear plane heat source only. There is an additional heat source, namely, frictional heat source at the chip–tool interface in metal cutting which contributes to the temperature rise distribution. This problem is addressed in Part II [26] of this three-part series. In fact, the actual temperature rise distribution will depend on their combined effect, namely, the shear plane heat source and the frictional heat source at the chip–tool interface, which is addressed in Part III [27].

Acknowledgements

This project was initiated by a grant from the NSF US–China co-operative research project on the Thermal Aspects of Manufacturing. One of the authors (R.K.) thanks Dr. Alice Hogen of NSF for facilitating this activity and for her interest in this project. The authors are indebted to NSF for their continuing support to one of the authors (R.K.) at OSU on the various aspects of the manufacturing processes. Thanks are due, in particular, to Drs. B.M. Kramer, Ming Leu, Delci Durham of the Division of Design, Manufacturing, and Industrial Innovation and to Dr. Jorn Larsen Basse of Tribology and Surface Engineering program. The author also thanks the MOST Chair for Intelligent Manufacturing for enabling the preparation of this paper. The authors also thank the reviewers for many valuable suggestions and comments which significantly increased the quality of the presentation.

Appendix A

As mentioned in the text we give $i(p, \xi)$ for $p < 0$ and $p > 0$ in this appendix A (Table 8, Fig. 15).

Table 8
Special function $i(p, \xi)$, $i(p, \xi) = \int_{u=0}^{u=\beta} e^{-u\xi} K_0(u)\, du$

(a) When $p < 0$

p	$i(p, 1.0)$	$i(p, 0.9)$	$i(p, 0.8)$	$i(p, 0.7)$	$i(p, 0.6)$	$i(p, 0.5)$	$i(p, 0.4)$	$i(p, 0.3)$
− 0.1	− 0.343	− 0.338	− 0.337	− 0.335	− 0.333	− 0.332	− 0.330	− 0.328
− 0.2	− 0.576	− 0.565	− 0.560	− 0.555	− 0.550	− 0.544	− 0.540	− 0.534
− 0.4	− 0.955	− 0.933	− 0.918	− 0.902	− 0.887	− 0.872	− 0.857	− 0.843
− 0.6	− 1.252	− 1.216	− 1.187	− 1.158	− 1.131	− 1.103	− 1.078	− 1.053
− 0.8	− 1.504	− 1.452	− 1.408	− 1.363	− 1.322	− 1.281	− 1.244	− 1.208
− 1.0	− 1.739	− 1.666	− 1.604	− 1.542	− 1.486	− 1.431	− 1.381	− 1.334
− 1.2	− 1.957	− 1.861	− 1.779	− 1.699	− 1.626	− 1.557	− 1.494	− 1.435
− 1.4	− 2.160	− 2.039	− 1.935	− 1.836	− 1.747	− 1.663	− 1.587	− 1.516
− 1.6	− 2.347	− 2.200	− 2.075	− 1.957	− 1.851	− 1.752	− 1.664	− 1.582
− 1.8	− 2.528	− 2.353	− 2.204	− 2.066	− 1.943	− 1.829	− 1.729	− 1.637
− 2.0	− 2.703	− 2.498	− 2.323	− 2.164	− 2.025	− 1.897	− 1.785	− 1.684
− 2.2	− 2.871	− 2.634	− 2.433	− 2.254	− 2.097	− 1.955	− 1.833	− 1.722
− 2.4	− 3.032	− 2.762	− 2.535	− 2.335	− 2.162	− 2.007	− 1.873	− 1.755
− 2.6	− 3.188	− 2.883	− 2.630	− 2.408	− 2.219	− 2.051	− 1.908	− 1.782
− 2.8	− 3.337	− 2.997	− 2.717	− 2.475	− 2.270	− 2.090	− 1.938	− 1.804
− 3.0	− 3.481	− 3.105	− 2.798	− 2.535	− 2.315	− 2.124	− 1.963	− 1.823
− 3.5	− 3.824	− 3.339	− 2.963	− 2.651	− 2.397	− 2.182	− 2.013	− 1.852
− 4.0	− 4.154	− 3.558	− 3.110	− 2.750	− 2.463	− 2.226	− 2.048	− 1.872
− 4.5	− 4.446	− 3.756	− 3.238	− 2.831	− 2.515	− 2.259	− 2.073	− 1.886
− 5.0	− 4.749	− 3.939	− 3.347	− 2.898	− 2.555	− 2.284	− 2.081	− 1.895
− 5.5	− 5.025	− 4.080	− 3.428	− 2.945	− 2.582	− 2.299	− 2.093	− 1.900
− 6.0	− 5.290	− 4.191	− 3.489	− 2.978	− 2.600	− 2.309	− 2.100	− 1.903
− 7.0	− 5.772	− 4.402	− 3.597	− 3.032	− 2.627	− 2.322	− 2.109	− 1.906
− 8.0	− 6.231	− 4.536	− 3.657	− 3.059	− 2.639	− 2.327	− 2.114	− 1.907

Table 8. (*Continued*)

(b) When $p > 0$

p	$i(p, 1.0)$	$i(p, 0.8)$	$i(p, 0.6)$	$i(p, 0.5)$	$i(p, 0.4)$	$i(p, 0.2)$
0.1	0.300	0.311	0.314	0.316	0.318	0.320
0.2	0.472	0.485	0.493	0.498	0.502	0.511
0.4	0.683	0.709	0.731	0.741	0.754	0.778
0.6	0.794	0.831	0.866	0.883	0.903	0.942
0.8	0.857	0.903	0.949	0.972	0.998	1.052
1.0	0.896	0.950	1.005	1.033	1.065	1.132
1.2	0.914	0.980	1.043	1.075	1.112	1.190
1.4	0.932	1.000	1.068	1.104	1.145	1.233
1.6	0.944	1.013	1.086	1.124	1.168	1.265
1.8	0.947	1.022	1.098	1.139	1.185	1.288
2.0	0.955	1.027	1.107	1.149	1.197	1.306
2.2	0.958	1.031	1.112	1.156	1.206	1.320
2.4	0.960	1.034	1.117	1.161	1.213	1.330
2.6	0.961	1.035	1.119	1.165	1.217	1.338
2.8	0.962	1.037	1.121	1.168	1.221	1.344
3.0	0.962	1.037	1.123	1.169	1.223	1.348

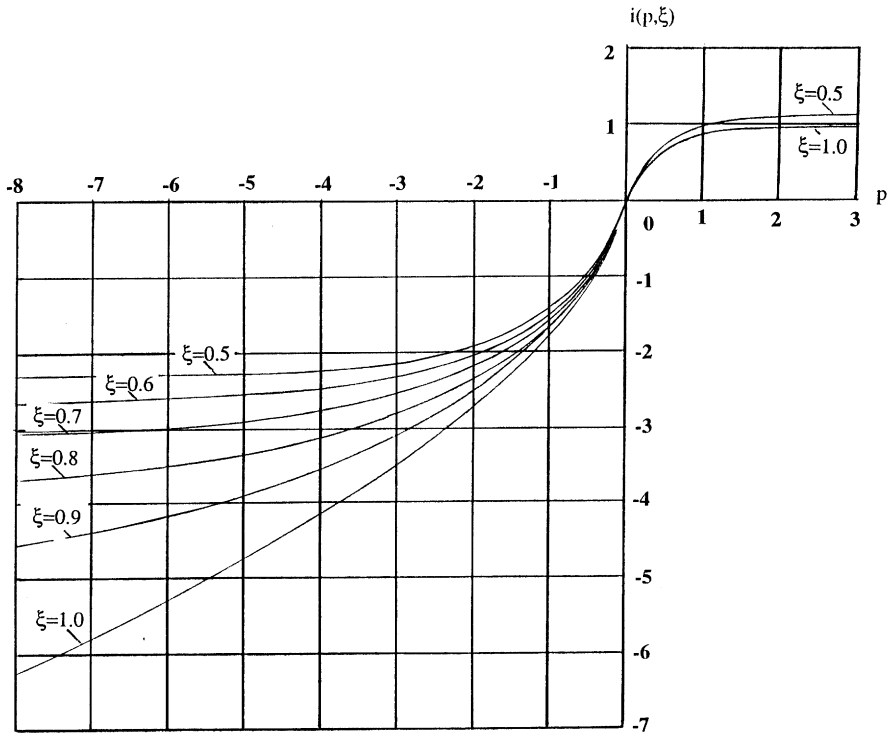

Fig. 15. Variation of the special function $i(p, \xi)$ with p for various values of ξ.

References

[1] Thompson B. Count Rumford. An inquiry concerning the source of heat which is excited by friction. Philosophical Transactions of the Royal Society of London 1798;18:278–87.
[2] Joule JP. Mechanical equivalent of heat. Philosophical Transactions of the Royal Society of London 1850;61–81.
[3] Taylor FW. On the art of cutting metals. Transactions of ASME 1907;28:31–248.
[4] Schmidt AO, Gilbert WW, Boston OW. A thermal balance method and mechanical investigation for evaluating machinability. Transactions of ASME 1945;67:225–32.
[5] Schmidt AO, Roubik JR. Distribution of heat generated in drilling. Transactions of ASME 1949;71:245–52.
[6] Gottwein K. Die Messung der Schneiden temperature beim Abdrehen von Flusseisen. Maschinenbau 1925;4:1129–35.
[7] Shore H. Tool and chip temperatures in machine ship practice. Massachusetts Institute of Technology Thesis, 1924.
[8] Rosenthal D. The theory of moving sources of heat and its application to metal treatments. Transactions of ASME 1946;68:849–66.
[9] Blok H. Theoretical study of temperature rise at surfaces of actual contact under oiliness lubricating conditions. Proceedings of General Discussion on Lubrication and Lubricants, Institute of Mechanical Engineers London, 1938. p. 22–235.
[10] Jaeger JC. Moving sources of heat and the temperature at sliding contacts. Proceedings Royal Society of NSW 1942;76:203–24.
[11] Hahn RS. On the temperature developed at the shear plane in the metal cutting process. Proceedings of First U.S. National Congress of Applied Mechanics, 1951. p. 661–6.
[12] Chao BT, Trigger KJ. The significance of thermal number in metal machining. Transactions of ASME 1953;75:109–20.
[13] Trigger KJ, Chao BT. An analytical evaluation of metal cutting temperature. Transactions of ASME 1951;73: 57–68.
[14] Loewen EG, Shaw MC. On the analysis of cutting tool temperatures. Transactions of ASME 1954;71:217–31.
[15] Leone WC. Distribution of shear-zone heat in metal cutting. Transactions of ASME 1954;76:121–5.
[16] Nakayama K. Temperature rise of workpiece during metal cutting. Bulletin of the Faculty of Engineering, National University of Yokohama, Yokohama, Japan, 1956;21:1–5.
[17] Boothroyd G. Temperatures in orthogonal metal cutting. Proceedings of the Institution of Mechanical Engineers (Lon) 1963;177(29):789–810.
[18] Weiner JH. Shear plane temperature distribution in orthogonal machining. Transactions of ASME 1955;77:1331–41.
[19] Rapier AC. A theoretical investigation of the temperature distribution in the metal cutting process. British Journal of Applied Physics 1954;5:400–5.
[20] Dutt RP, Brewer RC. On the theoretical determination of the temperature field in orthogonal machining. International Journal of Production Research 1964;4:91–114.
[21] Dawson PR, Malkin S. Inclined moving heat source model for calculating metal cutting temperatures. Transactions of ASME 1984;106:179–86.
[22] Barrow GA. Review of experimental and theoretical techniques for assessing cutting temperatures. Annals of CIRP 1973;22/2:203–11.
[23] Loewen EG, Shaw MC. Contributed to the discussion of Ref. [2], p. 116–7.
[24] Piispanen V. Theory of formation of metal chips. Journal of Applied Physics 1948;19:877–81.
[25] Tay AO, Stevenson MG, de Vahl davis G. Using the finite element method to determine temperature distributions in orthogonal machining. Proceedings of the Institution of Mechanical Engineers London 188;627.
[26] Komanduri R, Hou ZB. Thermal modeling of the metal cutting process, Part II Temperature rise distribution due to frictional heat source at the tool-chip interface, International Journal of Mechanical Sciences 1999, submitted.
[27] Komanduri R, Hou ZB. Thermal modeling of the metal cutting process, Part III Temperature rise distribution due to combined shear plane heat source and frictional heat source at the tool–chip interface. International Journal of Mechanical Sciences 1999 submitted.

[28] Taylor GI, Quinney H. The latent energy remaining in a metal after cold working. Proceedings of the Royal Society of London Series A 1934;143:307–26.
[29] Carlsaw HS, Jaeger JC. Conduction of heat in solids. Oxford, U.K.: Oxford University Press, 1959.
[30] Boothroyd G. Fundamentals of metal machining and machine tools. New York: McGraw-Hill Book Co, 1975.
[31] Shaw MC. Metal cutting principles. Oxford U.K.: Oxford University Press, 1984.
[32] Ueda T, Sato M, Nakayama K. The temperature of a single crystal diamond tool in turning. Annals of CIRP 1998;47/1:41–4.
[33] Merchant ME. Basic mechanics of the metal cutting process. Transactions of ASME 1944;66:A65–71.
[34] Hahn RS. Contributed to the discussion of Ref. [12], p. 115.